

A.I.F.A. - ITALIAN ASSOCIATION FOR FATIGUE IN AERONAUTICS
DEPARTMENT OF AEROSPACE ENGINEERING - UNIVERSITY OF PISA

Review of aeronautical fatigue investigations
carried out in Italy
during the period April 2007 - March 2009

by
L. Lazzeri
Department of Aerospace Engineering
University of Pisa - Italy

This document summarizes the main research activities carried out in Italy about aeronautical fatigue in the period April 2007 – March 2009. The main topics covered are: load monitoring, fatigue of metallic structures, damage in composites, full scale testing.

31st ICAF Conference, Rotterdam, The Netherlands, 25-26 May 2009

CONTENTS

	Page
1. INTRODUCTION	7/1
2. MEASUREMENT AND ANALYSIS OF OPERATIONAL LOADS	7/1
2.1 - AM-X life monitoring (Alenia Aeronautica)	7/1
2.2 - Life monitoring of the TORNADO fleet (Alenia Aeronautica)	7/1
2.3 - EF Typhoon life monitoring (Alenia Aeronautica)	7/1
2.4 - EF Typhoon usage data analysis (Alenia Aeronautica)	7/2
2.5 - MB-339 Aircraft (Alenia Aermacchi)	7/2
2.6 - Structural fatigue monitoring of the SF-260 aircraft (Alenia Aermacchi)	7/3
2.7 - Health and Usage Monitoring System for AW101 helicopter (AgustaWestland)	7/3
2.8 - Individual Aircraft Tracking Program of the C-27 J aircraft (Alenia Aeronautica)	7/4
3. METALS	7/4
3.1 - Fatigue behaviour of notched and unnotched materials	7/4
3.1.1 Fatigue behaviour of monolithic and metal laminate aluminium open hole specimens (Univ. Pisa)	7/4
3.1.2 Fatigue behaviour of structural items with un-removed corrosion (Alenia Aeronautica)	7/5
3.1.3 Fatigue of gears (AgustaWestland)	7/6
3.2 - Crack propagation and fracture mechanics	7/6
3.2.1 Damage Tolerance analysis of unitized structures (Univ. Pisa)	7/6
3.2.2 Development of a Flaw Tolerance helicopter fatigue design methodology (AgustaWestland)	7/8
4. COMPOSITES AND FIBER METAL LAMINATES	7/8
4.1 - Crack propagation monitoring using FBG sensors in CFRP specimens (Milan Polytechnic)	7/8
4.2 - Damaged anisotropic stiffened panels under cyclic compressive loads (Turin Polytechnic)	7/9
5. INTERNATIONAL AND NATIONAL RESEARCH PROGRAMS	7/10
5.1 - Clean Sky Joint Technology Initiative - European Technology Platform (Alenia Aeronautica)	7/10
5.2 - MAAXIMUS research (Alenia Aeronautica)	7/10
5.3 - OAST-OASB Fatigue Test Program (Alenia Aeronautica)	7/11
6. COMPONENT AND FULL-SCALE TESTING	7/11
6.1 - Development fatigue test of the M-346 wing (Alenia Aermacchi)	7/11
6.2 - M-346 Certification Full Scale and Component fatigue tests (Alenia Aermacchi)	7/12
6.3 - EF Typhoon (Alenia Aeronautica)	7/13
7. AIRCRAFT FATIGUE SUBSTANTIATION	7/13
7.1 - C-27 J program (Alenia Aeronautica)	7/13
7.2 - ATR 42- ATR 72 Ageing program (Alenia Aeronautica)	7/13
7.3 - Boeing B 787 – Fuselage Section 44-46 and Horizontal Tail Damage Tolerance design (Alenia Aeronautica)	7/13
7.4 - Development of the RRJ Superjet 100 (Alenia Aeronautica)	7/14
7.5 - A109 helicopter family (AgustaWestland)	7/14
7.6 - AW139 helicopter (AgustaWestland)	7/14
7.7 - AW149 development (AgustaWestland)	7/14
7.8 - NH90 (AgustaWestland)	7/14
7.9 - M-346 trainer (Alenia Aermacchi)	7/15
7.10- UAS Technology (Alenia Aeronautica)	7/16

	Page
8. OTHER FATIGUE INVESTIGATIONS OF GENERAL INTEREST, ALSO ON NON-AERONAUTICAL SUBJECTS	7/16
8.1 - Electric Strain Gauge Measurement of Residual Stress in Welded Panels (Univ. Pisa)	7/16
8.2 - Fatigue crack propagation in tensile shear stainless steel spot welded specimens (Univ. Pisa)	7/17
9. REFERENCES	7/17
FIGURES	7/18

1. INTRODUCTION

This paper summarises aeronautical fatigue investigations which have been carried out in Italy during the period April 2007 to March 2009. The different contributions have been arranged according to the topics, which are loading analysis, fatigue and fracture mechanics of metallic materials, fatigue behaviour of composites and full scale component testing. A list of references, related to the various items, is presented at the end of the document.

The review is based on the activities carried out within the various organisations belonging to A.I.F.A., the Italian Association for Fatigue in Aeronautics. The author gratefully acknowledges the fundamental contribution, which has made this review possible, given by several A.I.F.A. members, who are the representatives of Universities and Industries in A.I.F.A.

2. MEASUREMENT AND ANALYSIS OF OPERATIONAL LOADS

2.1 - AM-X life monitoring (Alenia Aeronautica)

The life monitoring program for the AM-X aircraft is an activity that has been in progress for a long time and regularly information has been given in the various National Reviews; it is based on classic mechanical g-meter readings and on information about configurations and mission profiles. With respect to the situation described in the last Review, where the data base included 158,000 flight hours, corresponding to 132,000 flights, the statistical population has increased, reaching 169,000 monitored flight hours (corresponding to 166,000 flights). The usage severity is measured by means of the Load Severity Index (L.S.I.), that is the ratio between the damage cumulated in a flight hour and the damage of an average hour of the reference spectrum. The analysis of the data, reported in fig. 1, is an update of the similar analysis carried out two years ago, and shows that the Load Severity Index (L.S.I.) average value (among all the fleet) results just above 1. Hence the fatigue life consumption has to be considered substantially in line with the design assumptions. Looking at the L.S.I. trend in function of time (fig. 2), it can be seen that, after it stabilized below 1, in the last 2 years the L.S.I. shows a barely rising trend.

2.2 - Life monitoring of the TORNADO fleet (Alenia Aeronautica)

Since the Tornado has entered into service with the Italian Air Force in 1980, the fatigue life monitoring of the IAF fleet has been performed by Alenia Aeronautica by means of its in-house developed computer program that utilizes mechanical g-meter readings together with configuration/masses control. In total, 240,000 flights hours (corresponding to 190,000 flights) have been monitored so far. Among the 5 (4 + 1 dummy) locations monitored by means of this Interim Monitoring System, the lower wing panel remains the most fatigue affected. However, the Load Severity Index, even with a small increase, is definitely below design values (Fig. 3).

Also on the basis of the low fatigue consumption rate, it was possible to extend (formally in February 2009), the aircraft life from 4000 up to 6000 Flight Hours. Anyhow, the individual tracking will be maintained, in order to assure a correct management of the fleet maintenance actions and to identify any possible anomalous fatigue consumption. At the same time, a re-organisation of the huge amount of qualification data cumulated during past years is in progress, together with other PANAVIA Partners, keeping all the modifications introduced into account. The re-assessment, performed for the Italian Air Force, of the entire structure against fatigue problems originated strategy and maintenance activities to extend the Italian aircraft life to 6000 Flight Hours. Moreover, a revision of the Maintenance Manual was performed and several operative supplements were issued. The avionics updating program on the aircraft, which will be maintained into service till 2025, is now in progress.

2.3 - EF Typhoon life monitoring (Alenia Aeronautica)

Since 2003 to now a total of 29 EF Typhoon aircraft (20 single seater and 9 twin seater) have been delivered to the Italian Air Force; at the end of 2005 the aircraft officially entered into IAF service, operational in the role of patrol and interception. Up to December 2008, the Italian fleet had performed a total of 7487 flights (corresponding to 9291 Flight Hours).

Alenia Aeronautica provides support to IAF for the Typhoon fleet fatigue and usage monitoring by means of the analysis of the data collected by the Structural Health Monitoring system (SHM). The SHM system supplies:

- the **Fatigue Index calculation** for 10 structural significant location: this value indicates the percentage of the design fatigue life that has been spent;
- the **Auxiliary Data** relevant to flight data (g, roll rate, Mach, weight, altitude, etc): these data are not directly used for fatigue calculations, but can be used for specific analyses;
- the **Event Monitor** that points out any significant structural event compared to pertinent envelopes.

Among the Auxiliary data, g exceedences are counted by a computer based algorithm which simulates the mechanical g-meter behaviour. In this way, it is possible to easily represent the in-flight recorded g-spectrum and compare it to the design one. At present, the usage shows a spectrum similar in shape to the one used in the design phase, but definitely less severe (Fig. 4). This trend finds a confirmation in the Fatigue Indexes calculations, that are below design too.

2.4 - EF Typhoon usage data analysis (Alenia Aeronautica)

An investigation is ongoing at Alenia Aeronautica for the study of the coupling of two basic parameters of the EF Typhoon usage, namely the load factor (N_z) and the roll rate. Data were collected from 7 IAF in-service aircraft (6 single seater and 1 twin seater), using the "auxiliary data" facility of SHM system. A poster will be presented at the ICAF 2009 Symposium, [1]. Some preliminary data emerging from the study allows the comparison between design hypotheses and in-flight measurements and is reported below.

Studying the N_z and roll rate coupled/uncoupled occurrences, it is possible to understand the effective in-flight behaviour of the aircraft in terms of symmetric and asymmetric manoeuvres and compare it to the original design assumptions.

Three types of manoeuvres have been assumed per design: the first one is completely symmetric (S), hence with only significant N_z and null roll rate. Asymmetric manoeuvres are indeed assumed significant if the roll rate is higher than 30 deg/s. Two types (fig. 5) of asymmetric manoeuvres were defined and called "Type A" and "Type B". The Type A consists of a roll to bank at $N_z=1g$ ("A" segment), pull to required N_z at null roll rate, return to $N_z=1g$ ("SA" segment) and finally roll out of bank at $N_z=1g$ ("A" segment again). Hence the Type A asymmetric manoeuvre is characterized by non concurrent significant values of N_z and roll rate. On the other side, the Type B asymmetric manoeuvre consists of a roll to bank at $N_z=1g$, starting to pull to $N_z>1$ before peak roll rate ("OS" segment) and reaching the required N_z when the roll rate is null; after the required $N_z>1$ phase ("SA" segment), the roll out starts when N_z is still at peak value, reaching the required roll rate at $N_z=1g$ and finally rolling back to straight level ("SO" segment). Hence the Type B asymmetric manoeuvre is characterized by concurrent N_z and roll rate.

Organizing the in-flight recorded data into matrix form, it is possible to read and distinguish the occurrences of any flight manoeuvre condition: each area of the matrix belongs to a specific manoeuvre (or segment of manoeuvre).

From the analysis it came out that asymmetric manoeuvres are 65% of total number of manoeuvres, against 67.7% assumed in the design phase. Moreover, asymmetric type B manoeuvres are 30% of all asymmetric ones, against 9% in design; within Type B manoeuvres, SO segments are only 11% of OS segments, while an equal number was obviously assumed in the design.

Hence from the analysis of this data it results that the number of asymmetric manoeuvres is in line with design assumptions while asymmetric Type B (or partially Type B) manoeuvres, compared to Type A, are more numerous than in design assumption. Very significant is the fact that OS parts are much more than SO parts, hence the entrance in the manoeuvre seems to be usually more aggressive than the exit: the very great part (90%) of Type B asymmetric manoeuvres are indeed flown as Type B (concurrent N_z and roll rate) only at the entrance and become Type A (non concurrent N_z and roll rate) while exiting.

2.5 - MB-339 Aircraft (Alenia Aermacchi)

The MB-339 trainer is one of the most successful products in the Alenia Aermacchi portfolio, in service in nine different nations. The 230 MB-339 built have accumulated over 600,000 flight hours experience worldwide. The Italian Air Force aerobatic team, the "Frecce Tricolori", operates the customised MB-339PAN version.

The main activity on the MB-339 program today consists in the monitoring of the fleet fatigue life consumption. Depending on the aircraft version, different monitoring systems (i.e. based on different principles) are used. In the frame of this activity, a procedure has been developed for the assessment of the fatigue life consumption for the non-monitored flight hours on individual aircraft basis. This method has been deemed necessary in the framework of the structural updating related to the MB-339 Mid Life Update program. The above-mentioned procedure is applied to those structural items not previously monitored by means of the Airborne Strain Counter (ASC).

The starting point for the calculation is the monitored flight activity relevant to a sample of aeroplanes. The relationship between flight hours and life consumption is considered univocal and a function of the load spectrum. This method allows to evaluate the mean fatigue life consumption rate, typical of the fleet, with the desired probability and confidence levels. Thus, with this above-mentioned rate, it is possible to calculate the fatigue life spent during the non-monitored activity for each structural item of each aircraft.

The statistical approach is simply based on a linear regression model. The calculation of the rate can be based on the entire fleet data or only on a sample, and can be different for any monitored structural item. The procedure is iterative: after having defined a first sample, statistical checks are performed to verify two conditions: first, if the sample can be considered representative of the whole population and, second, if the regression analysis is statistically meaningful. In

affirmative case for both conditions, the mean consumption rate is computed and used. Otherwise, if the result is negative, a new sample is defined and the procedure iterated. If it is not possible to identify a sample, the statistical approach is not applicable and conservatively the highest fatigue consumption rate in the fleet is applied, waiting for the collection of more data. If the sample is smaller than the total population, the rate applied in the life calculations is different from the mean rate calculated for the sample; this difference is necessary in order to guarantee a well-defined probability with a well-defined confidence level to find a mean rate outside the range of the fleet.

An example of the statistical data is reported in fig. 6.

2.6 - Structural fatigue monitoring of the SF-260 aircraft (Alenia Aermacchi)

Twenty-seven different military customers have already bought 880 SF-260 in all variants. The fleet has accumulated over 1,900,000 flight hours worldwide. Recent customers include the Italian Air Force, which ordered its fourth batch of thirty SF-260EA, the last production version of the aircraft with an avionics configuration tailored to its specification. The SF-260 flight characteristics and performances allow its use for screening student pilot candidates, while also covering effectively the entire primary training phase.

The main fatigue activity for this program has been related to the implementation of a dedicated tool for the structural fatigue monitoring of the SF-260EA. The procedure, tuned with the fatigue test of the wing longeron, processes the fatigue-meter data recorded on each aircraft and calculates the damage for the critical sections. The damage evaluation is performed with the Palmgren-Miner's rule and allows to determine the equivalent flight hours (EFH) spent by each aircraft. In addition to the recorded "g" level, i.e. the Nz exceedance spectrum, the procedure requires information related to the type of mission performed. The tool has been developed to manage different aircraft mission weights. Moreover the number of landing is recorded and processed.

The procedure is articulated in the following steps:

- a) the Nz occurrence spectrum is obtained from the recorded Nz exceedance spectrum;
- b) for each mission, the spectrum is randomised and then a transfer function (different for each aircraft mission weight) is applied to calculate the bending moment at the reference wing station, depending on the Nz value;
- c) the time history defined in the above-mentioned manner is then subjected to a rainflow counting in order to extract the bending moment cycles. The corresponding stress cycles are subsequently calculated and then the damage is evaluated for each monitored structural element.

The fatigue status of each aircraft can be quantified by the percentage of spent life, the equivalent flight hours consumption and the residual life. A graphical comparison between flight hours (FH) and equivalent flight hours (EFH) is also reported in order to visually highlight the spectrum severity with respect to the design conditions (fig. 7). Moreover, for each aircraft, the Nz exceedance spectrum and the bending moment spectrum (shown in fig. 8) after the rainflow counting application are reported.

2.7 - Health and Usage Monitoring System for AW101 helicopter (AgustaWestland)

A research program is in progress for the exploitation of AgustaWestland Enhanced Structural Usage Monitoring (ESUM) and Transmission Usage Monitoring (TUM) to improve the evaluation of fatigue loading spectra. These usage monitoring systems are installed on AW101 variants, AW139 and NH90.

A paper was presented at the RTO meeting in Montreal last year, [2], reporting details of a comprehensive exercise made on a preliminary set of recorded data from Danish Royal Air Force AW101 helicopters to validate usage assumptions made in the qualification. This exercise is based on a limited flight hour monitoring of an AW101 fleet.

Occurrences per each flight regime tend to converge to stable values as the number of hours increase from 150 hrs to 300 hrs. At least 300 hours of recorded data per aircraft are therefore recommended to monitor actual usage.

The design spectrum is subdivided into the following major flight conditions:

- ✓ Ground conditions (taxiing, ...)
- ✓ Take-off and landing (flare, ...)
- ✓ Hover (IGE, OGE, spot turns, ...)
- ✓ Climb and descent (transition to Vy, climb TOP or MCP, ...)
- ✓ Autorotation and related power-off manoeuvres
- ✓ Level flight (banked turns, pull-ups, control reversals, various flight speeds, ...)

Further split is done in specific flight regimes, as quoted in brackets, and subconditions per:

- Weight
- Longitudinal balance
- Altitude

A dedicated software, ESUM, runs on an on-board computer and can recognize each flight condition with the related sub-conditions and associated weight, altitude and longitudinal balance using the following data:

- ✓ Weight
- ✓ Longitudinal balance
- ✓ Altitude
- ✓ Speed
- ✓ Load factor
- ✓ Bank angle
- ✓ Longitudinal acceleration
- ✓ Climb and descent rate
- ✓ ACSR status

Plots of the distribution of various quantities, such as weight (fig. 9), centre of gravity position, altitude, etc, have been produced, as well as bank angle in a steady roll manoeuvre (fig. 10) and the level flight speed; this allows the identification of the most significant flight conditions and their relative occurrence frequency (fig. 11). The comparison of the flight conditions frequencies with the design assumptions can give a simple indication of the usage severity.

The same approach is being applied to the examination of data recorded on Canadian AW-101 helicopters.

2.8 - Individual Aircraft Tracking Program of the C-27 J aircraft (Alenia Aeronautica)

Fatigue life monitoring allows the operator to know the current status of its aircraft (in terms of Fatigue Residual Life and Crack Growth Residual Life), hence, to plan and optimise maintenance and usage of each aircraft inside the fleet. The C-27 J main Customers, to which the IATP program is applied, are:

Italian Air Force	11 Aircraft
Hellenic Air Force	10 Aircraft
Lithuanian Air Force	2 Aircraft
Bulgarian Air Force	2 Aircraft

About 10,000 Flight Hours have been achieved by the C-27 J fleet and a continuous monitoring by IATP program has been performed in order to track their *Structural Integrity* status. Information about the definition of the program are given in a past National Review, while a typical IATP output is shown in table I.

3. METALS

3.1 - Fatigue behaviour of notched and un-notched materials

3.1.1 - Fatigue properties of monolithic and metal laminate aluminium open hole specimens (Uni. Pisa)

Metal Laminate materials are produced by adhesive-bonding a number of thin sheets, to obtain the required thickness. These materials were developed in the '70s in The Netherlands and have subsequently been improved by adding fibres in the adhesive layer, giving rise to Fibre Metal Laminates (FML).

Metal Laminate (ML) materials show superior behaviour, with respect to fatigue crack propagation and fracture resistance, compared to standard monolithic plates, mainly due to the artificial obstacles in crack propagation represented by the different layers.

Comparative fatigue and crack propagation tests were carried out at the Department of Aerospace Engineering of Pisa on open hole monolithic and ML specimens. Monolithic specimens were machined starting from a 1.27 mm thick sheet. ML specimens were machined starting from a laminate made of four sheets of 2024-T3 aluminium alloy, thickness 0.3 mm, bonded by epoxy film Hysol EA 9657 adhesive.

Four groups of specimens were examined:

- Type A. Reference monolithic specimens, drilled and reamed individually (geometry in fig. 12). Gentle manual deburring was subsequently carried out.
- Type B. Monolithic specimens drilled and reamed by stacking ten specimens on the table of a milling machine; two thick aluminium plates were pressed against the package during machining, fig. 13. The holes were not deburred.
- Type C. Machined as specimens Type B, but inserting 0.15 mm thick plastic foils between the specimens, fig. 13. Also in this case, the holes were not deburred.
- Type D. Machined as specimens Type A, using the ML sheet. Gentle manual deburring was carried out after machining, obviously involving only the external laminae.

Specimens Type B and C simulate the internal laminae of a Metal Laminate, which cannot be deburred after drilling. Plastic foils were introduced in specimens Type C to simulate the presence of the adhesive in Metal Laminates, which is very soft in comparison to metal layers.

Fig. 14 shows the fatigue test results relevant to the three different monolithic specimens. The beneficial effect of hole deburring is clearly evidenced. The endurance limit decreases from 90 to 67 MPa, if deburring is not performed (specimens Type A and B). Even worse was the behaviour of the specimens Type C, drilled (and reamed) with interposed plastic foils (again, no deburring): in this case, the fatigue strength decreases to 58 MPa.

The results relevant to specimens Type A are compared in fig. 15 with those of specimens Type D. The improved behaviour of specimens Type D, made of ML material, is evident, even if deburring is obviously applied only on the two external layers; the allowable maximum fatigue stress for infinite life is about 100 MPa.

In addition to the fatigue behaviour, also the crack propagation of naturally nucleated cracks was investigated: after its natural initiation, a 0.5 mm corner crack was monitored. Fig. 16 shows the results of crack growth tests, carried out at $S_{max}=130$ MPa, $R=0.1$. Again, the results obtained show the better behaviour of ML specimens with respect to the monolithic ones, also from the crack propagation point of view.

The crack propagation life of a 0.5 mm corner crack was about 19300 cycles ($S_{max}=130$ MPa, $R=0.1$) in specimens Type A and about 107500 cycles in specimens Type D, tested under the same load conditions. At the same time, the total fatigue life, given in fig. 15, was about 150000 cycles in both specimens.

The main conclusion is that fatigue cracks nucleate earlier in ML specimens, but they propagate slower, so that the total fatigue life is quite similar. More details on this investigation can be found in [3].

3.1.2 - Fatigue behaviour of structural items with un-removed corrosion (Alenia Aeronautica)

Two research activities relevant to corrosion are now ongoing at Alenia Aeronautica within the TORNADO program: the first one on the behaviour of structures corroded and repaired, the second one on the changes of fatigue properties of items with un-removed corrosion. The need for the second investigation arose when corrosion traces were found in a scarcely accessible area of the wing diffusion member.

This activity has been performed through the following steps:

- Comparative tests between corroded and un-corroded coupons to identify fatigue performance degradations in presence of corrosion;
- Calculation of stress levels for different locations with corroded and un-corroded material;
- Definition of stress spectra for different selected locations;
- Fatigue calculations for corroded and un-corroded material;
- Identification of corrosion level in low K_t areas producing the same criticality of un-corroded holes.

To perform comparative tests, flat rectangular specimens with edge notches (fig. 17) have been used, for either un-corroded (with a thickness of 13 mm) and corroded material (starting from a thickness of 15mm in order to obtain 13mm after corrosion attack). The material used was 2024-T351.

Preliminarily, a conditioning activity was performed to statistically reproduce the same typology and depth of corrosion damage previously evaluated on lower wing panel (exfoliation corrosion – about 1 mm deep). The ASTM G 34 corrosion test procedure was used, defining the corrosive solution to be used for this purpose. The solution volume to metal exposed area ratio of 30 ml/cm² (200 ml/inch²) was selected: in this condition, a corrosion depth of about 1 mm is obtained after 8 days of continuous exposure to the corrosive agent.

From micrographic investigations at higher magnification, under the classical exfoliation macro-appearance (fig. 18), some presence of inter-granular corrosion (0.15 mm deep) has been found.

The Fatigue Loading Spectrum for the test was derived from the Tornado MAFT Nz spectrum, appropriately amplified in order to obtain a specimen life of about 16,000 hours and with the lower branch modified in order to avoid compression loads (fig. 19).

The tests performed on un-corroded specimens gave an average life of about 14,660 flight hours. The lives from each individual corroded specimen were normalized to a unique value of corrosion depth, i.e. the nominal 1 mm exfoliation for each face plus 0.15 mm of additional intergranular corrosion, to keep the effective corrosion scenario of each specimen into account. The normalizing factor was the result of the effective stress (based on the remaining area, measured with a 0.1 mm accuracy) and of the S-N slope. The normalized life goes from a minimum value of 1,460 to a maximum value of 2,750 normalized flight hours, with an average value of 2,066 normalized flight hours.

From the Crack Surface analysis of corroded specimens, an increase of inter-granular corrosion was noted at the edge of the masked area, that was the side face of the specimen (notch internal surface included). In order to evaluate this effect, two additional specimens were prepared: in the first one the notch radius was increased after the corrosion, removing the critical zone, while a thicker masking layer was applied to the second one before exposure to corrosive environment; the two additional specimens gave lives of 1727 and 2632 normalized flight hours, respectively.

Hence, according to test results, the Knock Down Factor due to the Exfoliation Corrosion results equal to

$$KF = \frac{\text{Fatigue Life}_{\text{uncorroded}}}{\text{Fatigue Life}_{\text{corroded}}} = 7 \div 8.5$$

This Knock Down Factor value was not expected. Alenia Aeronautica past experience on fatigue performance degradation of corroded materials refers to "Pitting corrosion", which is reducing fatigue life of 20÷25%.

Anyway, the MAFT successfully performed demonstrated that the wing has a life of 18,000 test hours also for geometries containing holes ($K_t=3$) and, assuming that the flat parts that originated this investigation had a K_t equal to 1.5, a life increase of an order of magnitude can be considered demonstrated.

Finally the trend of fatigue life degradation in corroded material due to the stress increase caused by thickness reduction has been investigated and a comparison was made with the life of uncorroded holes. It was possible to conclude that a stress increase of 1.8 times (corresponding to a reduction of the thickness of about 45%) on a flat part (supposed characterized by a K_t equal to 1.5) would lead to the same life of the un-corroded holes (included in the MAFT test). In other words, even in presence of a large thickness reduction, the critical section remains the neighbouring un-corroded holes.

3.1.3 - Fatigue of gears (AgustaWestland)

A relevant cooperation with Milan Polytechnic – Dept. Mechanical Engng. started more than 4 years ago to improve the evaluation of root bending fatigue of AgustaWestland gears; some details have already been given in the last National Review.

A summary paper was presented in 2008 at AGMA Technical Meeting, [3], reporting high cycle fatigue of case carburized gears (see Table II). A second set of tests was completed on 4 configurations of nitrided steel gears but data analysis is still in progress.

The extensive campaign on carburized materials has given precise information on the fatigue limits of the four groups tested, both in absolute and relative terms. Analysis of the results with different S-N curve shapes (GEAR05 and GEAR06 in fig. 20) improves the definition of the fatigue strength in the 10^5 cycles region, important for transient power regimes and overtorque analysis.

The fatigue strength of the 4 configuration of carburized gears was investigated in Phase 1 of the project, where all the tests were carried out up to 10 million cycles, using 102 gear tooth specimens, for a comprehensive amount of 434 million cycles. In Phase 2 of the project, tests were performed up to 100 million cycles, using 8 specimens for one single material configuration, for a comprehensive amount of 734 million cycles. The tests performed at very high number of cycles confirm the shallow shape of the S-N curve, estimated on the basis of shorter tests, fig. 21.

The test procedure developed has now become the standardized approach at AgustaWestland to evaluate, compare and qualify new materials, new processes and new designs.

Additional tests are now in progress for low cycle fatigue evaluation and block spectrum fatigue using an hydraulic rig. The purpose is to confirm the S-N curve shape in the high load region (10^4 - 10^5 cycles) and the applicability of Miner's rule for finite life assessment.

Another activity is in progress to improve AgustaWestland fatigue analysis of gears. Two modules are almost ready and the relevant software is in the debug phase. They cover:

- a) gear 'standard' fatigue analysis using flight recording from rotor mast or engine inputs;
- b) gear fatigue analysis using HUMs power spectra recordings.

The third module will be based on the detailed stress analysis of the gear tooth for the bending loading cycle. The task developed with Milan Polytechnic will take into account the different loading environment in gear tests at amplified loading and the service power spectra, addressing practical improvements or unnecessary conservatism.

3.2 - Crack propagation and fracture mechanics

3.2.1 - Damage Tolerance analysis of unitized structures (Uni. Pisa)

The major objective of the DaToN project, partly funded by the EU within the 6FP, was the development and validation of damage tolerance analysis methodology for integrally stiffened panels produced by means of new, advanced technologies. For this purpose, a large test programme has been carried out by various partners of the Consortium (FOI, NLR, DLR, EADS IW Suresnes and Ottobrunn, IAI, and the Universities of Brno, Porto, Sheffield and Pisa) on specimens manufactured by means of the following technologies:

- 1) High Speed Machining, i.e. fully integral panels
- 2) Friction Stir Welding.

3) Laser Beam Welding.

Stiffened panels with a fixed geometry, reported in fig. 22, were manufactured by means of the three technologies above mentioned, in order to highlight the influences of the various processes on Fracture Mechanics properties. For the Laser Beam welded configuration, two slightly different variants were realized, which differed one from the other for the location of the weld bead: in LBW1 panels the joint was a corner laser welding between the stringer and the skin, while the LBW2 panels had a welded butt joint between the stringer web and the stringer feet, obtained by machining the starting sheet.

In the Friction Stir Welded panels the stringer and the skin were joined in a T configuration, with the tool working from the flat side.

The panels were manufactured in 2024 and 6056 alloys, provided by Alcan in different thicknesses and heat treatments. In total, almost 120 panels were manufactured, i.e. 30 samples for each configuration (as explained before, two configurations were laser welded). The panels were distributed to the various partners in order to allow the execution of the tests and their repetition (to gain confidence in the results) in a relatively short time.

The experimental activity performed at the Department of Aerospace Engineering of Pisa was composed by fatigue crack growth tests and measurement of residual stresses on welded stiffened panels. The crack propagation tests program performed in Pisa is summarized in Table III. The panels are identified by the base material and the production technology utilized.

The HSM panels tested in Pisa were made of 6056-T651, machined starting from a 30 mm thick plate. On the contrary, the welded panels tested in Pisa were made of both alloys investigated in the project, namely 2024 and 6056. Alcan provided 2024-T3 sheets and 6056-T4 sheets, that were used for manufacturing the welded panels. In the case of this last material, two procedures were followed: 1) weld the sheets in the -T4 condition and later submit the welded panel to an ageing to -T6 condition by artificially aging at 190°C for 4 hours (this is indicated by PWHT, i.e. Post Welding Heat Treatment); 2) heat treat the -T4 sheets to -T6, weld and test in the as-welded condition (in this case, no indication is added to the test name).

Constant amplitude crack propagation tests were carried out, using two different load conditions:

- 1) $S_{\max} = 80 \text{ MPa}$, $R = 0.1$
- 2) $S_{\max} = 110 \text{ MPa}$, $R = 0.5$.

The initial crack was introduced in the centre of the panel and so the problem investigated was the crack approaching and crossing a stringer.

The results of the crack propagation tests are reported in the graphs of figs. 23-26, in terms of mean value of the crack length versus number of cycles (small differences were observed between the flat side and the stringer side, as a consequence of the secondary bending present in the crack pane, due to the eccentricity of the centre of gravity position). The experimental results were reported to the same initial crack length to correctly compare them.

In fig. 23 the results relevant to different 6056 panels are reported, all tested at 80 MPa and $R = 0.1$, and in fig. 24 the results of the tests at 110 MPa and $R = 0.5$.

It is possible to notice how in both cases the residual stress that are present in the welded panels slow down the crack propagation rate with respect to the HSM panels. As a matter of fact, in this particular configuration, the crack spends a large part of its life in the centre of the bay, where the compressive residual stress field has a beneficial effect.

Crack propagation results from laser beam welded panels in 2024-T3 are compared in figs. 25-26, at the two stress ratios and levels, 80 and 110 MPa. The behaviour is quite similar, as an obvious consequence that the differences between LBW1 and LBW2 panels are very small.

Another interesting observation is that the crack growth resistance of 6056 is comparable to the one of the well-known 2024, as shown for example in fig. 27.

The 6056 material allowed the opportunity to assess the influence of two different heat treatment and manufacturing procedure: a very similar behaviour was observed in the 6056 panels tested in the “*as welded*” condition (starting from sheets in a -T6 condition) with respect to the panels welded in -T4 and afterwards subjected to an extra heat treatment, PWHT.

Another important activity was focused to the assessment of the residual stresses in the welded panels, which is always a complex problem. The Department of Aerospace Engineering of the University of Pisa has gained a certain experience in the experimental evaluation of residual stresses using a destructive sectioning method. After having bonded strain gauges on the panel, these are zeroed and then cuts of progressively increasing length are introduced in the panel: this allows the relaxation of the internal residual stress. By measuring the difference between the final relaxed state and the initial configuration it is possible to obtain the residual deformation present on the panel.

In the experimental activity on the DaToN panels most attention was paid to the evaluation of the residual stress acting in the longitudinal direction, i.e. the stringer direction, the most important from a practical point of view because it is superimposed to the stress deriving from the external load.

It should also be considered that the residual stresses are not constant during the component life and re-distribute as crack grows. The present activity had the objective of measuring the initial stress field, at the beginning of the test.

Each panel analysed was instrumented by 62 strain gauges, positioned in couples (back-to-back) on both skin panel sides and on the stringer web too. The strain gauge map is reported in fig. 28, with the strain gauge numbers from 0 to 61. In total, seven panels were instrumented for measuring the longitudinal residual stress field. Figs. 29-30 show two examples, relevant to 2024-T3 panels: FSW and LBW2.

3.2.2 - Development of a Flaw Tolerance helicopter fatigue design methodology (AgustaWestland)

This topic was also included in previous editions of the Italian National Review, because AgustaWestland has a long term research program in progress on the applicability of the Flaw Tolerance EASA CS 29 requirements. AgustaWestland preferred method for compliance with Flaw Tolerance requirements for dynamic components is the adoption of the “no damage growth” concept.

The typical flaw size assumed is a corner or a semi-circular crack of radius $r = 0.38$ mm, for parts exposed to accidental damage in flight, and a smaller flaw of radius $r = 0.25$ mm for parts protected in flight, after maintenance inspections. As far as the no-growth concept is concerned, it is applied through the use of the Kitagawa-Takahashi diagram. For this purpose, a Flaw Tolerance Data Base (FTDB) is being progressively extended, within a collaboration with Milan Polytechnic - Dept. Mechanical Engng.; it is a valuable tool for design, verification and demonstration of compliance with DT requirements. The latest data, produced in the last two years, are Kitagawa diagrams and crack growth data for high strength steels for transmission shafts and gears.

An additional task was started last year on the combined effects of shot peening on fatigue endurance and threshold for crack propagation. Tests were carried out on Al 7475, subject of a paper for ICAF 2009 [3], and an extensive activity is in progress on other alloys used for rotor mechanical parts and primary structural components (Ti-6Al-4V, Al 7050, PH steels ...). Some results are shown in figs. 31-32.

Access to Kitagawa diagrams and threshold data for flaw tolerance is managed by a dedicated software which provides guidance for proper usage and protects proprietary data. A new release 2.0 of the software is planned this year, fixing some minor bugs, increasing robustness and incorporating all improvements highlighted during the comprehensive validation process.

4. COMPOSITES AND FIBER METAL LAMINATES

4.1 - Crack propagation monitoring using FBG sensors in CFRP specimens (Milan Polytechnic)

In the last few years, a research activity is in progress at the Department of Aerospace Engineering of Milan Polytechnic, focused on the development of methods and techniques for the Structural Health Monitoring (SHM) of composite smart structures.

Taking the advantage of the small diameter and the high sensitivity of the Optic Fibre Sensor, Fiber Bragg Gratings (FBG) have been embedded in carbon fabric (Cytec T800/X01) composite laminates for the delamination detection over the DCB test. During the test, data, such as strain and spectrum of FBG, are recorded by OTTO, a passive interrogator unit, and OSA, an optical spectrum analyzer. A FE model, able to simulate the damage propagation in the material, allows to recover strain distribution in the embedded grating position (fig. 33).

Such strain distribution is the input of FBGSim program, developed in Matlab, that simulates the reflection spectrum of FBG. The obtained numerical spectra have been compared with the experimental ones. By coupling FBGSim to a genetic algorithm it is possible to recover strains from the spectrum (fig. 34). The changing shape of the spectrum, as well as the variation of the strain distribution along the grating, are effective indicators of crack propagation. The capability of the FBG sensor to monitor both the mean strain along the grating and its distribution represents an interesting issue for structural health monitoring systems (SHM).

The FE model used to correlate the strain distribution measured by the optic fibre sensor is based on cohesive material models to represent interlaminar layers between the plies of a composite laminate. The adopted technique is based on a structural idealisation of the laminate consisting of lumped normal stress carrying areas, modelled by bi-dimensional elements, connected to solid elements capable to transmit the shear stress that correctly restores the equilibrium conditions in the layers within the laminate [5]. All the adopted elements are characterized by physical properties of the composite material of the laminates, both in terms of toughness as well as of stiffness. Such approach is able to overcome some numerical difficulties relevant to the conventional cohesive model schemes. These schemes are based on zero-thickness interface elements and theoretically infinite stiffness is required. The FE model has been validated considering interlaminar fracture characterisation tests to establish Mode I (DCB test) and Mode II (ENF test) interlaminar fracture toughness of carbon fabric (Hexcel AS4/8552) and unidirectional (Hexcel IM7/8552) composites (Fig. 35 and 36).

The developed approach has also been adopted to model the growth of the interlaminar damage in carbon composite specimens impacted at low energy level ($8 \text{ J} \div 30 \text{ J}$). Figure 37 shows the C-Scan pictures of a 20 J impact on three UD specimens and the results of the corresponding numerical analysis. Investigations are carried out to study the influence

of the strain rate sensitivity of the interlaminar properties as well as the demand to further develop the model by including in-plane damage mechanisms.

The possibility to numerically analyse the onset and the development of interlaminar damage in such tests represents a fundamental benchmark to investigate the damage tolerance of composite materials [6], providing a very important issue to develop efficient damage tolerant composite structures, thus reducing the great amount of experimental tests usually required.

4.2 - Damaged anisotropic stiffened panels under cyclic compressive loads (Turin Polytechnic)

Stiffened panels are commonly used for their efficiency in developing high buckling resistance, also in the case of composites. A skin delamination or a stringer de-bonding in a stiffened panel can cause buckling to occur at a load lower than the design critical load and cause a reduction in global strength. Local/global critical behaviour is modified by the presence of a damage, such as de-bonding between skin and stiffeners. In these cases, it is important to assess and characterize the damage, as well as to identify the progression of damage under application of cyclic loading and the residual structural strength.

A research activity has been carried out at the Department of Aerospace Engineering of the Turin Polytechnic, focused on the evaluation of damage effect on the critical and post-critical behaviour of flat stiffened composite panels, subjected to cyclic compressive loads. Attention was paid, in particular, to the possible identification of damage growth under cyclic in-plane compressive loads capable to induce post-critical conditions, with the aim of identifying and determining specific formulations for problems of structural damage propagation.

The activity was partially supported by the Italian Ministry of University project devoted to “Fully Composite Fuselage for Medium and Large Pressurized Aircraft” and was composed by a first numerical design phase, followed by the manufacturing of a stiffened panel and its test. The machine for the experimental activity is available in the Department of Aerospace Engineering of the Turin Polytechnic and is capable to apply a combined biaxial compression and shear loading to rectangular flat panels of 1000x700 mm maximum dimensions. The testing machine has the possibility to apply cyclic loading conditions at different frequency in longitudinal and transverse directions. An anisotropic stiffened panel has been designed, containing an artificially induced damage: skin-stiffener de-bonding. This damaged panel has been numerically studied in order to evaluate and compare its structural behaviour with experimental results.

a) preliminary numerical analysis. An M40 carbon epoxy flat panel, reinforced with blade stiffeners with an artificially simulated defect (skin-stiffener de-bonding) was numerically investigated. The stiffener width and height was 30 mm, with the following laminate lay-ups: $[(+45)_2/0_2/(+45)/90_2]_s$ for the panel, $[(+45)_2/0_6/(+45)/0_2]_s$ for the stiffener cap and $[(+45)_2/0_6/(+45)/0_7]_s$ for the stiffener web. The panel average thickness was 2.8 mm, and overall panel dimensions were 1000x700 mm. Three load conditions were considered in this preliminary numerical analysis: uniaxial compression and two biaxial cases, with an overall load per unit length ratio of 0.15 and 0.2 (N_y/N_x , transversal to longitudinal). A damage in the form of de-bonded length was considered and three types of damages were analytically studied: type A damage was a de-bonding length of 100 mm in the central part of one stiffener, type B duplicates the same de-bonding in the central part of two stiffeners, while type C considers a de-bonding length of 200 mm in the central part of one stiffener. The C-type damage induces an evident local buckling in the de-bonded area at a load level compatible with the experimental machine capability and with a well pronounced skin buckling. Type-C configuration was therefore chosen for the configuration to be tested, with a damage extension of 220 mm.

The longitudinal load applied to the models for the biaxial cases was twice the critical load for the integer skin (so producing a clear post-buckling behaviour), while for the uniaxial compression case the longitudinal load was limited to 400 kN, considered sufficient for damage activation. The numerical analyses on defective panels under biaxial compression showed an evident buckling of the skin (unsupported in the damage area) at a load level of about 0.72 times the maximum load (400 KN). As a conclusion of this preparatory activity, it is important to point out that in the uniaxial case a buckling is expected to occur with a well pronounced shape. In the biaxial case the occurrence of buckling is not so evident and a damage-global buckling coupling seems to occur at high applied load.

b) experimental static behaviour. A flat stiffened panel was manufactured for the test activity. Several strain gages were bonded back-to-back along the mid-line and the quarter-line panel position. A biaxial compression test was performed first, with the application of a load per unit length ratio N_y/N_x of 0.15. The aim was to detect the activation load for the local debonded skin deflection. The numerical-experimental longitudinal strain comparison revealed the tendency of the panel to undergo out-of-plane displacement in the direction of the stiffener side, so avoiding the buckling of the damaged area (fig. 38). A subsequent uniaxial compression test was performed. The experimental results demonstrated the activation of damage deflection at a load level of about 0.52 times the maximum load (400 KN). The restoring curve proceeds along a different path up to a load ratio of about 0.42 where it remains over the previous loading one. The snap local buckling effect was very clearly shown in the test, and also detected by the strain gauge measurements.

c) preliminary fatigue results. A preliminary fatigue test was planned, under application of uniaxial compression, with occurrence of buckling at every load cycle. The load frequency was quite low (0.1 Hz), in order to make easier the

observation of the damage behaviour. The load cycle varied between 0.5 and 0.6 times the maximum load (400 KN). The cycling curves follow the “after snap” path, as indicated during the static phase. Very small variation in equivalent stiffness was determined according to the results of strain gauge measurements. The strain gauges close to the defect point showed a bit higher variation in their measurements, which was directly connected with a change in damage dimension during cyclic loading. The snap condition seemed slightly modified in strain behaviour as a result of damage accumulation: higher strain was detected for the same load level after snap. This effect increased with the number of cycles (fig. 39). Numerical analysis of the observed phenomena is in progress.

5. INTERNATIONAL AND NATIONAL RESEARCH PROGRAMS

5.1 – Clean Sky Joint Technology Initiative - European Technology Platform (Alenia Aeronautica)

The purpose of this research, partly funded by the European Union within the 7th Framework Program, is to demonstrate the validity and the degree of maturity of the aeronautical technologies developed with the goal of reducing the pollution due to the air traffic.

The project is based on six platforms (in brackets the leaders):

- ✓ Green Regional Aircraft (Alenia Aeronautica);
- ✓ Smart Fixed Wing Aircraft (Airbus & SAAB);
- ✓ Green Rotorcraft (Agusta Westland & Eurocopter);
- ✓ Sustainable and Green Engine (Rolls-Royce & Safran);
- ✓ Systems for Green Operations (Thales & Liebherr);
- ✓ Eco-Design (Dassault & Fraunhofer Institut).

The objective of the Green Regional Aircraft platform is to develop a new generation Regional Aircraft that includes enhanced technologies for :

- ✓ More efficient aerodynamic configuration
- ✓ Weight reduction (minimum 9% less)
- ✓ New generation engine (10-20% fuel reduction)

In addition to the development of the new technologies for the achievement of the above mentioned objectives, the project comprises the validation of a demonstrator up to flight test; an existing platform will be modified to receive panels and components where the developed technologies will be implemented and integrated. The objective of the Flight Test will be to obtain an in-flight validation for the advanced structural technologies that require data acquired in a real operating environment. Strains measured in the full scale test and in-flight will be compared.

5.2 - MAAXIMUS Research (Alenia Aeronautica)

The MAAXIMUS acronym stands for **M**ore **A**ffordable **A**ircraft Structure Lifecycle through **eX**tended, **I**ntegrated, & **M**ature **nU**merical **S**izing and this project, partly funded by the European Union within the 7th Framework Program, consists of a key enabler for drastic changes in the development of a mature virtual product sizing technology.

The objectives are quite ambitious and can be summarized in the following points:

- Structure **development cost** reduction of 5-10% (more mature technologies, less unexpected failures, lower number of tests, ...);
- Structure **development lead time** reduction of 10-20% (reduced time to introduce new technologies, less test, lean & efficient processes);
- Structure **direct operation cost** reduction of 5% (structure weight reduction: lighter materials, reduced conservatism, optimised designs, etc);
- Structural **maintenance cost** reduction of 5-10% (reduction of unexpected maintenance, extended life cycle, delayed planned maintenance, focused/anticipated maintenance).

Alenia Aeronautica’s contribution to the research is focused on:

- ✓ Automation in the assembly: monolithic structures
- ✓ Virtual structural sizing
- ✓ Repair numerical simulation
- ✓ Virtual testing techniques

In this project, “virtual testing techniques” refers to all the disciplines, included fatigue design. The activities are focused also on smart materials (for durability assessment) and Health Monitoring, that have important implications for the fatigue management.

5.3 - OAST-OASB Fatigue Test Program (Alenia Aeronautica)

Alenia needs to substitute the traditional but low environmental friendly OAC (Chromic acid oxidation) process with the more ecological ones OAST (sulphur-tartaric acid) or OASB (sulphur-boric acid).

A large experimental fatigue test campaign has been planned, composed by about 700 tests, to assess the influence of the new processes on the fatigue behaviour and to generate design allowables, on the following basis:

- ✓ 3 Kt values (Unnotched, 1.5, 3.0)
- ✓ 3 specimen thickness

In figure 40 the typical coupon shape and dimensions are shown. The fatigue test results should be available at the end of the year 2010.

6. COMPONENT AND FULL-SCALE TESTING

6.1 - Development fatigue test of the M-346 wing (Alenia Aermacchi)

The test, carried out on the LH prototype wing, started in October 2005 and was completed in May 2007, after 13560 simulated flight hours (SFH), when damages were found on a main structural item. As far as the monitored sections of the structure are concerned, applying the appropriate test spectrum severity index (ranging from 1 to more than 2) and scatter factor, almost all of them have nearly reached the design fatigue life.

The main objectives of the test were to verify the predictions about the location of the critical areas (and to highlight any other unpredicted criticality), to validate the analysis tools throughout correlation with test results (both for crack initiation and crack propagation analyses) and to test and validate the ForceMate® fatigue enhancement process. Finally, the test findings have been used to assess the fatigue behaviour of the wing for the series configuration.

The test article was mounted on a rig representative of the fuselage side from a configuration standpoint. The wing box and the trailing edge surfaces were loaded by means of a total of 16 actuators that reproduced the load distribution for the different 200 load conditions of the test spectrum, that was a flight-by-flight sequence of the manoeuvres performed by the aircraft; a random load history covering 200 FHRS has been defined in order to simulate a complex load sequence. The spectrum has been manipulated in terms of occurrences in order to reduce the test duration, generating, in the monitored sections of the structure, fatigue severity indexes greater than one.

Periodic inspections have been carried out in order to check fatigue critical areas and to give as much information as possible about propagation of nucleated cracks.

During the test, evidences were collected regarding fatigue damages developed at locations that were already highlighted as possible crack initiation sites, so confirming the criticality of these features and, through an analytical correlation with the series configuration, the improvements already introduced after the fatigue evaluation of the prototype configuration were positively assessed.

In addition to the predicted critical locations, only one further hot spot was identified during the test; the problem was solved by means of a modification introduced in the series configuration, followed by a final assessment and freezing of the wing.

In the following, some of the test findings will be described in detail.

- A crack, starting from the lower skin radius at the section between flap and spar (fig. 41) has been found. This feature was already identified by analysis as a possible critical location, due to the low value of the radius, that generates a high stress concentration; for this reason, the series configuration had already been improved, increasing the radius. The test demonstrated a good correlation between predicted and experimental results, for what concerns the crack initiation analysis. During the continuation of the test, crack propagation data was collected and compared with the analytical results obtained by means of a detailed finite element model simulation and a Nasgro® crack growth calculation; the analysis was quite conservative with respect to the real growth.
- Cracks were found at the main spars root, in the area between wing-to-fuselage attachment lugs and spar caps. See fig. 42 for example. Even this area was highlighted by analysis as a possible criticality, so that it had already been modified in the series configuration, increasing the thickness of the bracket and the value of the radius. The consequent decrease of the local stresses has been assessed by means of detailed finite element analyses.

- Cracks were found at two web holes of the front spar (fig. 43 and fig. 44).
For what concerns the circular hole (fig. 43), the anchor nuts holes have been identified as the main causes of the crack initiation. The investigation performed after the finding highlighted a quite high fatigue severity index of the test spectrum with respect to the design flight one, and the reason was an actuator too close to the critical areas. This assessment, together with the good correlation found between the updated analytical evaluation and the experimental results, has led to the conclusion that this section was not to be considered a real criticality with respect of the design flight spectrum.
As far as the rectangular hole with round corners is concerned (fig. 44), similar conclusions have been drawn.
- Cracks were found in the root zone of the forward main spar, in particular:
 - at fastener holes on the lower cap (fig. 45)
 - at the elliptical web hole (fig. 46), emanating from the edge at 45° with respect to the hole axes.An updated detailed finite element model has been developed in order to evaluate the stress state at the elliptical hole edge and the load transfer between the lower cap and the skin; the fasteners were modelled by means of the MSC/Patran Utility “Fastener Builder”.
Adequate correspondence has been found between analysis and experimental results as far as the crack initiation analysis is concerned.
This area was considered critical, due to load introduction and presence of stress concentration. The series configuration had been already improved, increasing the thickness of the cap and the web at hole edge, based on the results of the preliminary analysis of the prototype configuration.
- Two cracks have been found at the fillet radius between the cap and web of the spar carrying the two trailing edge flap attachments (fig. 47).
Evidence of fretting was discovered in the area. The investigation highlighted the presence of cracks also on the skin below the spar cap, emanated from the anchor nuts installation.
This section was the only one not previously considered among the theoretical analysis criticalities.
Because of the high local stress and the crack initiation and propagation, the conclusion has been drawn that a low cycle fatigue phenomenon has occurred. The design of the series configuration has been improved, stiffening the section and reducing the local stress.

After the completion of the test, a tear down inspection has been performed in order to investigate more deeply the findings of the test and to identify other possible hot spots. The wing has been disassembled and the critical items have been subjected to non-destructive controls. The components to be inspected have been selected on the basis of their structural criticality (primary load paths and local load introduction), of the analysis performed before the beginning of the test (theoretical critical locations) and of the test findings.

The dye liquid penetrant and the eddy current inspections have been mainly used, because the wing has a metallic structure; ultrasonic and radiographic inspections have been performed for particular cases, such as for flap and aileron assemblies, as they are full-depth honeycomb structures with metal to metal bonded joints.

The main test findings have been more deeply investigated also carrying out a fractographic analysis. In particular, the forward main spar has been thoroughly analysed, because of the presence of cracks:

- at the connection between wing-to-fuselage attachment lug and cap bracket (fig. 42);
- at fastener holes on the lower cap (fig. 45) in the root zone;
- at the elliptical web hole at the root area (fig. 46).

In conclusion, the objectives of the test have been fully achieved: the critical areas previously assessed by analysis were confirmed by the test findings, validating the analysis process too. In this way, the possibility to find fatigue problems on the main structural components of the wing for the series configuration is highly reduced.

6.2 – M-346 Certification Full Scale and Component fatigue tests (Alenia Aermacchi)

The Full Scale Fatigue Test (FSFT) will comprise the fuselage and the wings, including the leading edge flaps (i.e. nose droops) but not the trailing edge flap and the aileron, that will be separately tested, as well as the vertical and horizontal tails. The loads introduced on the FSFT by these components will be applied using suitable dummies/tools or directly by actuators acting on their aircraft structure attachments.

The design inertial and aerodynamic loads, typical for each fatigue load condition, will be introduced basically by means of actuators along the fuselage and the wing to generate the test load conditions. The locations and the entity of applied forces are evaluated with the aim to simulate as closely as possible the design internal forces and moments distribution. The equivalent damage approach, applied to the “control points”, defined during the Durability assessment, will give the final validation about the test load conditions.

The same approach will be applied for the component tests.

The non-stationary (buffet) load spectra will be applied basically with two different approaches:

- Quasi-static approach, introducing loads by means of actuators; the dynamic contribution is superimposed to the static one. This procedure will be followed for the FSFT and, partially, for the horizontal tail.
- “Pure” dynamic approach, exciting the structure normal modes involved in the buffet phenomenon by means of shakers, appropriately applied to the item. This procedure will be followed for the vertical tail and, partially, for the horizontal tail.

6.3 - EF Typhoon (Alenia Aeronautica)

The Production Major Airframe Fatigue Test (PMAFT) is now ongoing within BaeSystems facilities at Brough (UK). At the moment 6000 Flight Hours have been simulated (with design spectrum). Alenia Aeronautica is involved in this full scale test for the components under its responsibility and for the definition of buffet load spectra. In the test, buffet loads are treated separately for the fin and for the wing: fin buffet is introduced every 3000 SFH by means of the dedicated arrangement of a dynamic stinger (and in this phase of the test, the test article is modified in the rig, installing dummy engines to simulate the engine inertia characteristics and disconnecting the load actuators in the wing), while the wing buffet is simulated every 6000 SFH in a quasi static manner, with a loading spectrum defined on the basis of the equivalent fatigue cumulative damage. A poster presented at ICAF 2007 was dedicated to describe the methodology followed by Alenia Aeronautica in defining the fatigue damage associated to buffet conditions, [7].

7. AIRCRAFT FATIGUE SUBSTANTIATION

7.1 – C-27 J program (Alenia Aeronautica)

The C-27 J aircraft is a derivative of the Alenia G222/C27A aircraft modified to meet expanded or more stringent system-level requirements as determined primarily by market assessments and certification requirements. The main modifications, with respect to the G222, are related to the new engine installation (new engine nacelle design) and to the new landing gear design.

The certification basis is EASA CS 25, for European Customers, and FAR 25 amendment 87 for USA Operators.

JCA (Joint Cargo Aircraft) is the name of the US version of the C-27 J. The Fatigue and Damage Tolerance Design and Certification (according to FAR 25 regulation) have been completed. The first aircraft has been delivered to the USA Customer on October 2008.

Information about the Individual Aircraft Tracking Program has been already given in section 2.8 of this Review.

7.2 - ATR 42- ATR 72 Ageing program (Alenia Aeronautica)

The ATR Ageing Structures Program has the goal to extend the Airframe Service Life from 70,000 flights (the original Design Service Goal) to 105,000 flights. The ATR Fleet has reached about 10 Millions Flight Hours. The current life of the Fleet Leader Aircraft is about 60,000 Flights (corresponding to about 50,000 Flight Hours). All the activities necessary for the *Life Extension* have been completed and presented to the Airworthiness Authority: a description of the activities planned was presented at the ICAF Symposium in Naples, [8].

The Official Certification of the Extended Life is expected before the end of 2009.

ATR 72 - TMPA (Turkish Maritime Patrol Aircraft) Program

The Structural Design, Analysis and Certification were carried out for a Maritime Patrol version of the ATR 72, requested by the Turkish Air Force. New Damage Tolerance Analysis is in progress according to the dedicated Maritime Patrol mission profiles and mixing, as defined by the Customer.

7.3 - Boeing B 787 – Fuselage Section 44-46 and Horizontal Tail Damage Tolerance design (Alenia Aeronautica)

Information about the level of involvement of Alenia Aeronautica in this program was already given in the last Review. Here, it is important to recall that, together with the design, Alenia is in charge of the Fatigue/Damage Tolerance analysis and certification of the components under its responsibility. For the fuselage section, the design and manufacturing are Alenia’s responsibility, while the testing is planned in Boeing facilities. As far as the horizontal tail is concerned, Alenia is in charge for the performance of its Static and Fatigue Test.

The Composite (Main Box) Horizontal Tail Full Scale Fatigue Test was completed, after demonstration of three lifetimes with BVID damages, under a load spectrum amplified by a Load Enhancement Factor equal to 1.15; the test was concluded by a Residual Strength Test up to Ultimate Load. Fig. 48 shows a picture of the test article and set-up.

The metallic parts are being qualified by means of a Full Scale Fatigue Test, that is in progress on the complete Horizontal Stabilizer structure (left and right semi-tails assembled together, by means of metal fittings); the test article contains also metallic parts (Full HT including even the elevators and, obviously, also the relevant metallic interfaces). The load spectrum has been modified consequently, with respect with the one used in the test on the composite structure, mainly for the clipping and omission levels. The test is in progress: one lifetime has been completed (out of the three planned); fig. 49 shows a picture of the test set up.

7.4 - Development of the RRJ Superjet 100 (Alenia Aeronautica)

At the end of the year 2006 year, the cooperation with the Russian Industry SCAC (Sukhoi Civil Aircraft Corporation) was launched in Alenia, for a common activity related to the Design, Analysis and Manufacturing of the RRJ Superjet 100, fig. 50.

Alenia has performed the Fatigue Design of the rear fuselage, the rear pressure bulkhead and both the empennages. The prototype was rolled out from Sukhoi Komsomolsk-on Amur factory on 26 September 2007. The first flight was successfully accomplished last May 19, 2008.

7.5 - A109 helicopter family (AgustaWestland)

A109SP, a new version of the A109, has been derived from the "Grand" and is characterized by a large use of composite materials for the fuselage structure.

The certification program has required a full load survey, to validate the design load spectrum and the performance of a wide static and fatigue test campaign for the composite airframe parts.

7.6 - AW 139 Helicopter (AgustaWestland)

The civil certification of the AW139 helicopter has further been developed with:

- 6800 Kg ETOW (extended take off weight);
- Goodrich dual rescue hoist.

A load survey has been performed, dedicated to the weight extension, for acquiring dynamical loads; then additional limitations to be introduced in the Airworthiness Limitation Section of the Maintenance Manual have been assessed, both in terms of fatigue life reduction and inspection intervals for the damage tolerant parts.

The dual rescue hoist is designed for human usage and therefore it has been subjected to evaluations for fatigue life and Damage Tolerance according to the FAR/JAR 29.865(f) requirement, with analysis and tests on the support and back-up structure.

Moreover, Safe Life and Damage Tolerance evaluations are now completed for the certification process expected in 2009:

- **90 m rescue hoist breeze**, structural verifications for the rope length increment from 75 to 90 m;
- **Full ice**, test on heated blades with anti-ice system and load survey in Duluth (USA) to verify the loads in ice conditions;
- **19000 ft IGE altitude**, evaluation of take-off and landing loads due to an extension of the maximum altitude in ground effect.

7.7 - AW149 development (AgustaWestland)

AW149 is a new model in the development phase, for which the design criteria for fatigue and damage tolerance have been defined; a first detailed definition of the usage spectrum is in progress.

7.8 - NH90 (AgustaWestland)

NFH, the NH90 Navy Variant, will be fully qualified this year, after having completed most of the related activities between 2007 and 2008 for load survey and tests, including ship trials, high altitude, rescue and cargo hoists.

7.9 - M-346 trainer (Alenia Aermacchi)

M-346 is the Alenia Aermacchi Advanced/Lead-In Fighter Trainer, designed to allow the accomplishment of all the needs in Phase III and Phase IV of a military pilot training. The M-346 Durability and Damage Tolerance assessment proceeded in the last two years covering the activities related to development and qualification. Information has already been given in sections 6.1 and 6.2 of this Review about a development fatigue test performed on a prototype LH wing and on preparation activities for the Full Scale Fatigue Test on the series configuration.

The design spectrum has been updated on the basis of the results of the load survey activity performed on prototypes 1 and 2. The analytical verification of the airframe is now being iterated with the current data and the full scale fatigue test is being designed in order to verify the structure capability versus the new spectra. Fatigue and Damage Tolerance criteria are applied following the military international regulations, such as JSSG-2006.

In the framework of this activity, the following subjects have been developed:

- Analytical methodologies development, with particular reference to buffet and flight-by-flight spectra generation;
- Structural Durability and Damage Tolerance assessment, in particular regarding the process of definition of a restricted number of load conditions representative of the whole flight-by-flight spectrum.

7.9.1 – Analytical methodologies development

Structural fatigue analysis under buffet conditions is carried out in the frequency domain, i.e. by means of the definition of the Power Spectral Density (PSD) function, which gives a statistical representation of a stationary random process. In particular, the input is given in the form of a PSD of load and the structure is modelled by a linear transfer function relating the input forces to the output stresses at a particular location, so that the output from the model is expressed as a PSD too. The output may be any meaningful quantity, not necessarily a stress, but always in the form of a PSD.

A so-called “modal displacement method” has been defined and implemented in order to perform structural buffet analysis. For each normal mode of the structural items involved in the buffet phenomenon, a dedicated “static” loading for the finite element model has been defined. These loadings represent the modal deformation of the structure, i.e. the modal displacements normalized with respect to a reference point are applied to the FE model. Once the section to be analysed has been identified, the stresses (or any other quantity) for each “modal” loading are extracted: they represent the “form functions” used to generate the PSD of stress (or any other quantity) at the sections being analysed. The final PSD is calculated as a kind of “modal superposition” in the frequency domain, because it is given by the contribution of each PSD of the normalised modal displacement “weighted” with the stress related to the corresponding mode.

The above-described procedure has been implemented in a MatLab® routine that performs the PSD calculation taking as input the stresses (or any other quantity) related to each mode directly in a MSC/Patran text output and the PSD of displacements in a text format. The output is the PSD of the quantity under analysis, in text and graphical format (fig. 51).

The transformation from the frequency domain to the time domain, in order to define a stress sequence for the performance of the fatigue analysis, is made defining the Probability Density Function (PDF) of the stress ranges. This function gives the probability of a stress range to occur during the phenomenon, and so provides the number of occurrences of the range itself in a given period of time. The evaluation of the PDF is important, because different formulations can lead to quite different results: the one applied for M-346 buffet analysis is the Dirlik equation. Also this part of the procedure is implemented in the same MatLab® routine, that again generates text and graphical outputs (fig. 52). After having calculated the stress PDF, the corresponding spectrum of stress amplitudes with related occurrences is determined and, after the superimposition to a mean “static” component, if there is any, the complete spectrum can be defined.

The buffet contribution to the fatigue spectrum is assessed for the mission segments and the points-in-the-sky that show flight parameters such that the dynamic unsteady phenomenon is triggered.

While from a crack initiation point of view the buffet contribution to damage can be evaluated apart from the one due to the “static” manoeuvres (i.e. the traditional events included in a fatigue spectrum), since Miner’s rule is applied, and then the two are added together, the same is not feasible in the crack propagation analysis, where cycle sequence is fundamental for the crack growth.

For this reason, the following procedure has been implemented: first local flight-by-flight (FxF) stress spectra are generated, then the buffet contribution is insert exactly when performing the manoeuvre that triggers the phenomenon. The local FxF spectrum is a stress history, that is processed by a rainflow algorithm to extract the fatigue cycles potentially causing structural damage.

When a crack propagation analysis has to be carried out with a buffet contribution, the buffet spectrum evaluated with the above-mentioned PSD/PDF procedure is inserted at the correct point of the sequence, after application of the rainflow counting method; the counting algorithm maintains the sequence of the extracted cycles.

7.9.2 – Structural Durability and Damage Tolerance assessment

A restricted number of load conditions representative of the whole flight-by-flight spectrum has been identified. This process has been deemed necessary because the application of the conditions related to all the points-in-the-sky and the corresponding manoeuvre/gust events to the global finite element model of the aircraft would have been too time consuming. For this reason, the loads at defined aircraft stations have been calculated for each point-in-the-sky and for any kind of manoeuvre/gust characteristic for the point itself. On the basis of the loads values and of their evolution during the event, significant conditions and instants have been identified and then applied to the FE model.

An example of the above-described procedure is reported in fig. 53. In this case, the manoeuvres highlighted in bold are the chosen ones, basically based on the values of bending moment acting on wing and horizontal tail.

The total number of load cases determined in this way is 400. The definition of the load cases for the FE model has been the basis for the Durability and Damage Tolerance assessment and for the design of the fatigue tests.

7.10 - UAS Technology (Alenia Aeronautica)

In the last years Alenia Aeronautica was strongly interested in the UAS (Unmanned Aerial System) technology development. The main UAS's programs in which Alenia was involved are:

- ✓ SKY – X for basic technology demonstration;
- ✓ SKY – Y for MALE (Medium Altitude Long Endurance) technology;
- ✓ Molynx – Civil UAV for Control and Surveillance;
- ✓ Neuron – European UAS technology demonstrator.

Within the international Neuron program, Alenia has the primary responsibility for:

- ✓ Sonic Fatigue Design;
- ✓ Glass Window Design and manufacturing under Damage Tolerance Residual Strength requirements

The Sky-Y MALE Technology Demonstrator is a dedicated platform for validating several key enabling technologies for the surveillance in either military and civil operational scenarios. A picture taken during its first flight (June 2007) is shown in fig. 54.

8. OTHER FATIGUE INVESTIGATIONS OF GENERAL INTEREST, ALSO ON NON-AERONAUTICAL SUBJECTS

8.1 - Electric Strain Gauge Measurement of Residual Stress in Welded Panels (Univ. Pisa)

Residual stresses play an important role in the damage tolerance analysis of welded structures and, therefore, experimental measurements are of great interest. Sectioning of a strain gauge instrumented plate is a simple method to assess the residual stress in a welded plate.

At the Department of Aerospace Engineering of the University of Pisa, within the framework of a collaboration with Thales Alenia Space, measurements were carried out on a butt-plasma welded 2219-T851 aluminium plate, dimensions 550x890mm, thickness 7 mm. The strain gauge measurement was limited to one half of the panel only, fig. 55, assuming a symmetric distribution of the residual stresses. The first limit of the sectioning method is the distance between the cut line and the position of the strain gauges: this distance obviously cannot be zero and it must be compatible with the dimension of the strain gauges.

In order to relax completely the internal stresses, two cuts were performed, one in front and one at the rear of the strain gauges. The residual stress determined by elaborating only measurements of longitudinal deformations was practically equal to the one determined by combining the longitudinal and transversal strains. As a consequence, the experimental activity can be simplified by assuming that the transversal residual stresses are negligible and therefore only the longitudinal strain gauges can be used under this hypothesis.

The sectioning method of residual stress measurement was evaluated numerically using the commercial finite element code ABAQUS, by simulating the welding process in the plate. The 2219-T851 temperature dependent material properties were introduced as an input. The numerical analysis was divided in two stages: a thermal analysis was followed by a mechanical static stress analysis. The thermal analysis results were inserted in the mechanical static stress analysis in order to obtain the residual stress field in the model.

The obtained numerical results, fig. 56, compare well with the experimental ones, fig. 57. The effect of the partial or total relaxation of the residual stresses (one or two cuts), observed in experiments, was also observed in the numerical analyses. The effect of the distance of the cut from the position of strain gauges was evaluated using the same model; the results obtained show that the selection of such distance is not a critical issue, within reasonable limits.

Further details can be found in reference [9].

8.2 - Fatigue crack propagation in tensile shear stainless steel spot welded specimens (Univ. Pisa)

Fatigue tests were carried out on 4 mm thick spot welded joints, made of stainless steel AISI 301, quarter hard. Some specimens were instrumented with a strain gauge bonded in correspondence of one of the edges of the spot weld, fig. 58. The strain gauge output proved to be a reliable tool to monitor the nucleation and propagation of fatigue cracks, because a good correlation was found between strain gauge output and spent fatigue life, fig. 59. Some fatigue tests were suspended when the strain gauge output was equal to pre-fixed values, which corresponded to a fatigue life consumption in the range from 15 to 85%; then, the specimens were dissected to observe fatigue cracks. A good correlation existed also between crack depth and fatigue life. Small cracks were observed in specimens fatigue tested up to only 15% of the mean fatigue life; their nucleation can be estimated to have occurred between 5 and 10% of the fatigue life.

Finite Element calculations were carried out, introducing in the models cracks similar to those observed in the fatigue tests. The calculated strain at the external surface compared well with the measured strain, as a function of crack depth. The calculations demonstrated that small errors in strain gauge position can be tolerated without appreciable deterioration in crack dimension prediction.

More details can be found in [10].

9. REFERENCES

- [1] T. Giacobbe, F. Sardo: "Load Factor (Nz) / Roll Rate: First Comparisons between Design and In-flight Recorded Data on Eurofighter Typhoon Italian Fleet", Poster to be presented at the 25th ICAF Symposium, Rotterdam, 27-29 May 2009.
- [2] U. Mariani, R. Molinaro, B. Maino, S. Mancin: "Structural Usage Monitoring for Helicopter Fatigue Durability Validation" in RTO-MP-AVT-157 "Military Platform Ensured Availability", Proceedings of the RTO AVT Symposium held in Montreal (Canada), October 2008.
- [3] A. Lanciotti, C. Polese: "Fatigue properties of monolithic and metal laminated aluminium open hole specimens", *Fatigue and Fracture of Engineering Materials and Structures*. Vol. 31, n. 10, 2008, pp. 911-917.
- [4] G. Gasparini, U. Mariani, C. Gorla, M. Filippini, F. Rosa: "Bending Fatigue Tests of Helicopter Case Carburized Gears: Influence of Material, Design and Manufacturing Parameters", AGMA Fall Technical Meeting 2008.
- [5] A. Airoidi, G. Sala, P. Bettini, "Evaluation of Numerical Approaches for the Development of Interlaminar Damage in Composite Laminates", Proceedings ICCM-16, Kyoto Japan, 18-22 July 2007, pp. 1-10.
- [6] G. Sala: "Impact behaviour of heat-resistant toughened composites", *Composites, Part B* 31 (2000), 161-173.
- [7] G. Patrucco, T. Giacobbe, M. Colantuono: "Treatment of Buffet Phenomenon in Fatigue Analysis and in Fatigue Test on Military Aircraft", in Proceedings of the 24th ICAF Symposium, Pacini Editore, 2008, pp. 1084-1090.
- [8] A. Minuto, M. Cajani: "Atr 42/72 Ageing Program Finalised to the Airframe Life Extension", in Proceedings of the 24th ICAF Symposium, Pacini Editore, 2008, pp. 322-339.
- [9] G. Ivetic, A. Lanciotti, C. Polese: "Electric Strain Gauge Measurement of Residual Stress in Welded Panels", *The Journal of Strain Analysis for Engineering Design*. Vol. 44, n. 1, January 2009, pp. 117-126.
- [10] A. Lanciotti, C. Polese: "Fatigue crack propagation in spot welded joints", *Fatigue and Fracture of Engineering Materials and Structures*. Vol. 31, n. 1, 2008; pp. 76-84.

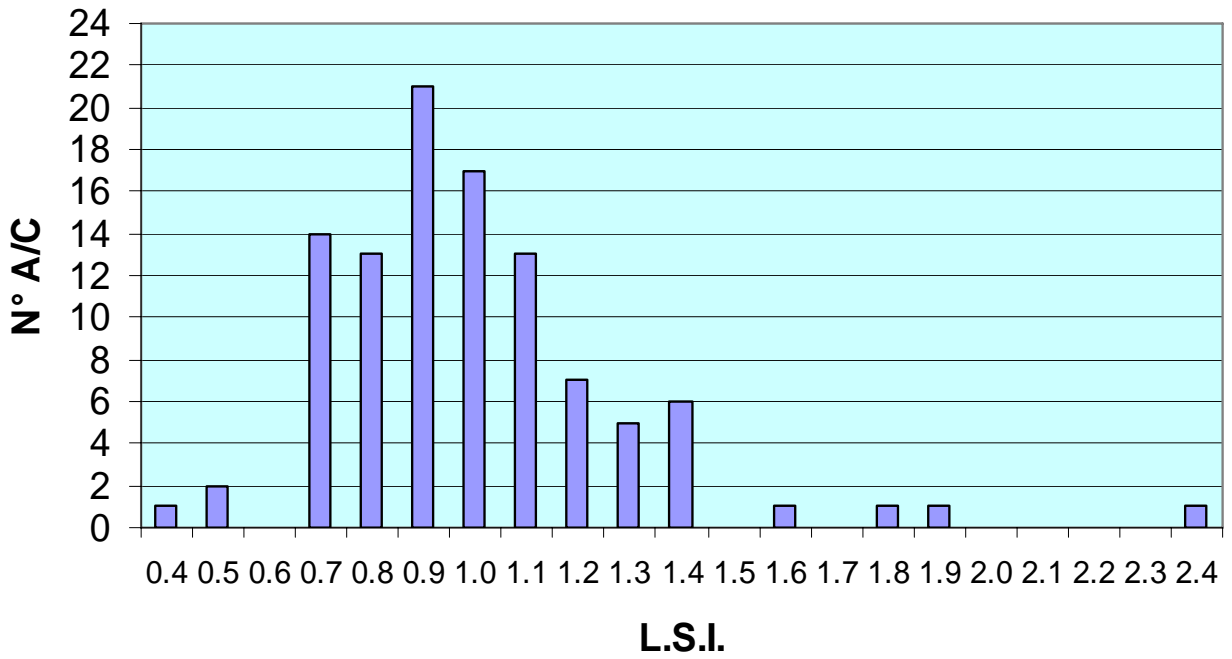


Fig. 1 – Load Severity Index distribution for the AM-X fleet.

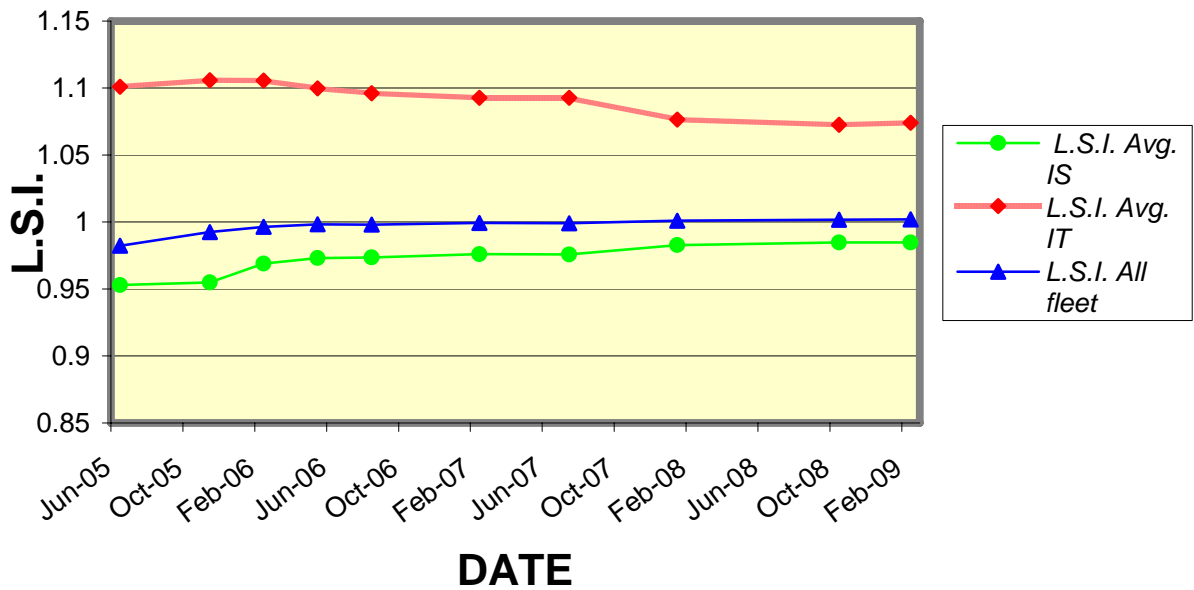


Fig. 2 – Trend of LSI relevant to the AM-X fleet

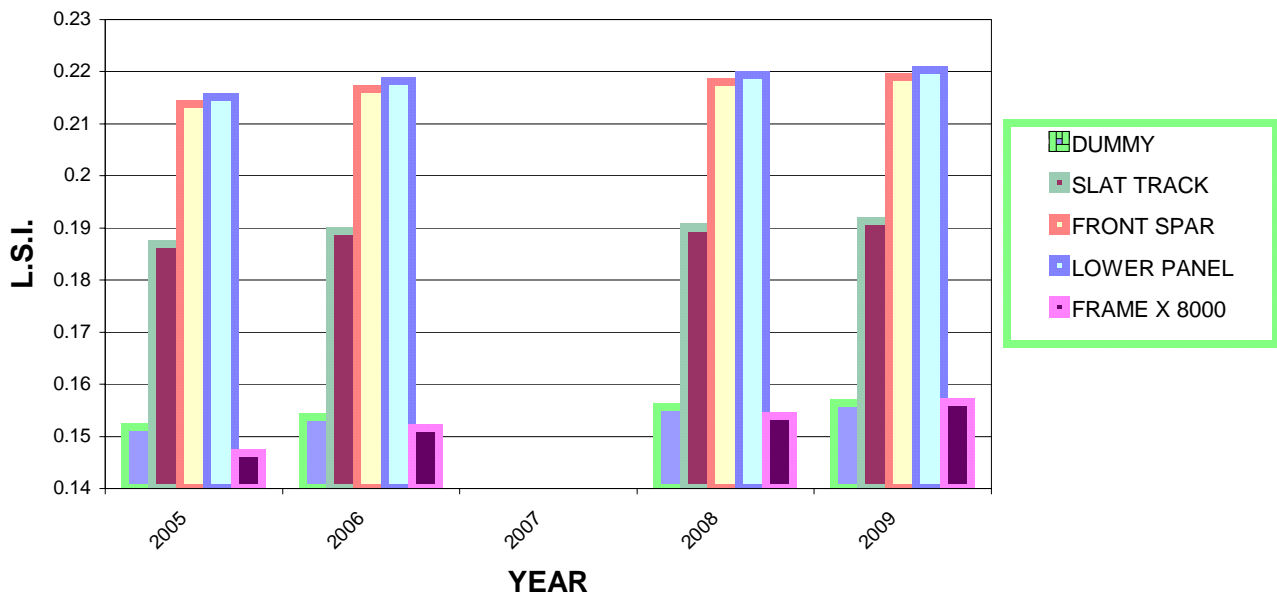


Fig. 3 - Load Severity Index trend for the monitored locations of I.A.F. Tornado fleet.

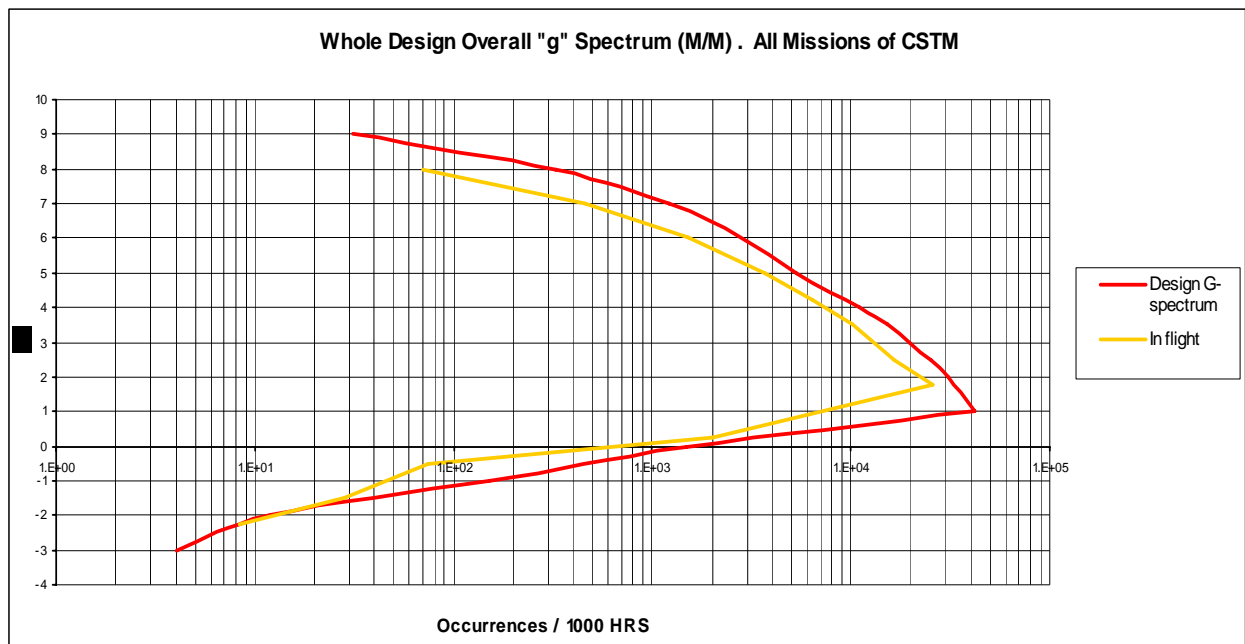


Fig. 4 - Normal acceleration usage spectrum vs. design spectrum for IAF Typhoon aircraft. (CSTM = Composite Set of Training Missions, i.e. a mix of all the mission types)

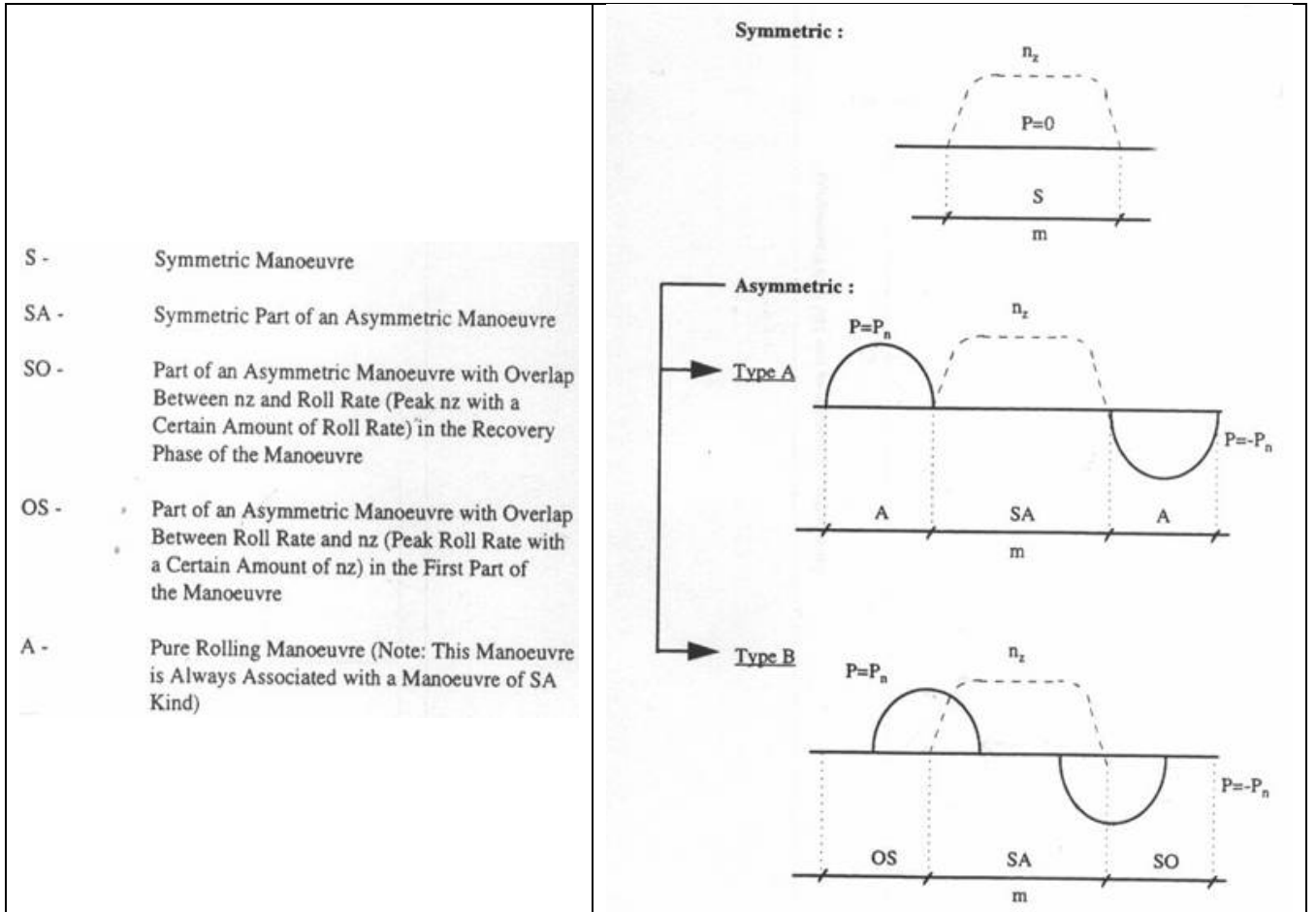


Fig. 5 – EF Typhoon Structural Health Monitoring: idealization of manoeuvres.

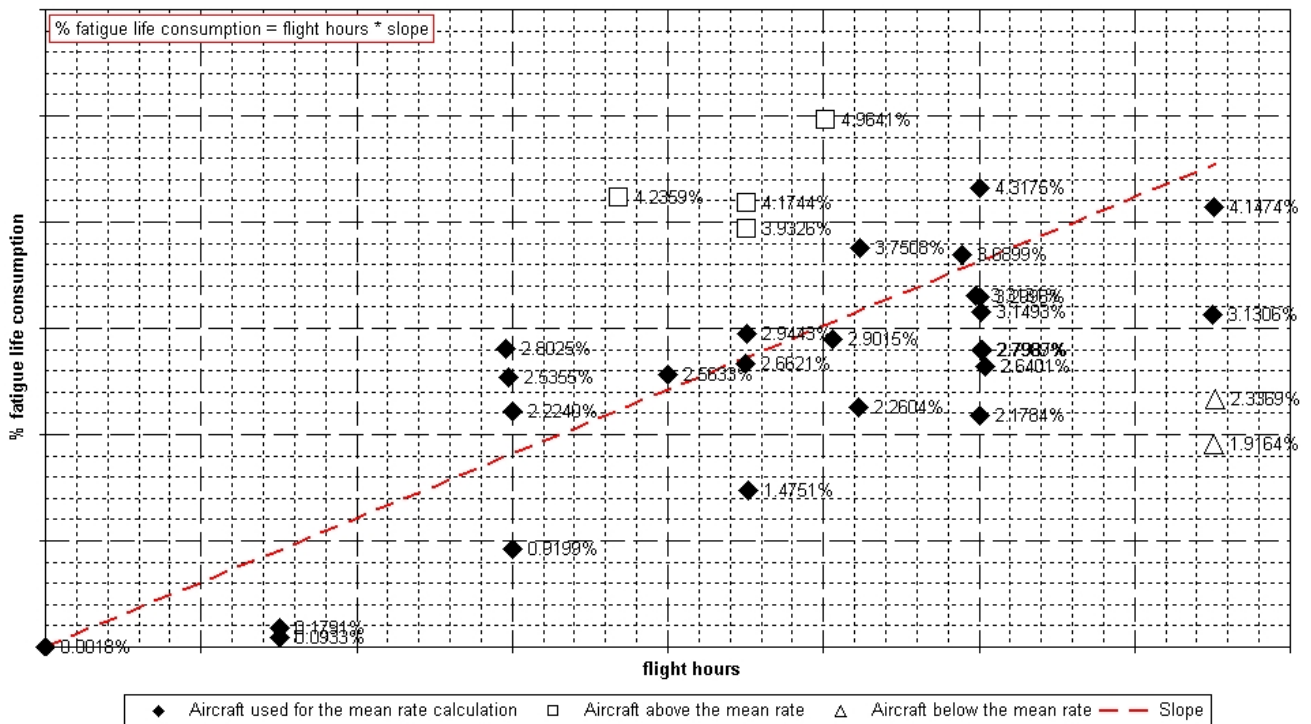


Fig. 6 - MB-339 assessment of the fatigue life consumption for the non-monitored flight hours; example of linear regression.

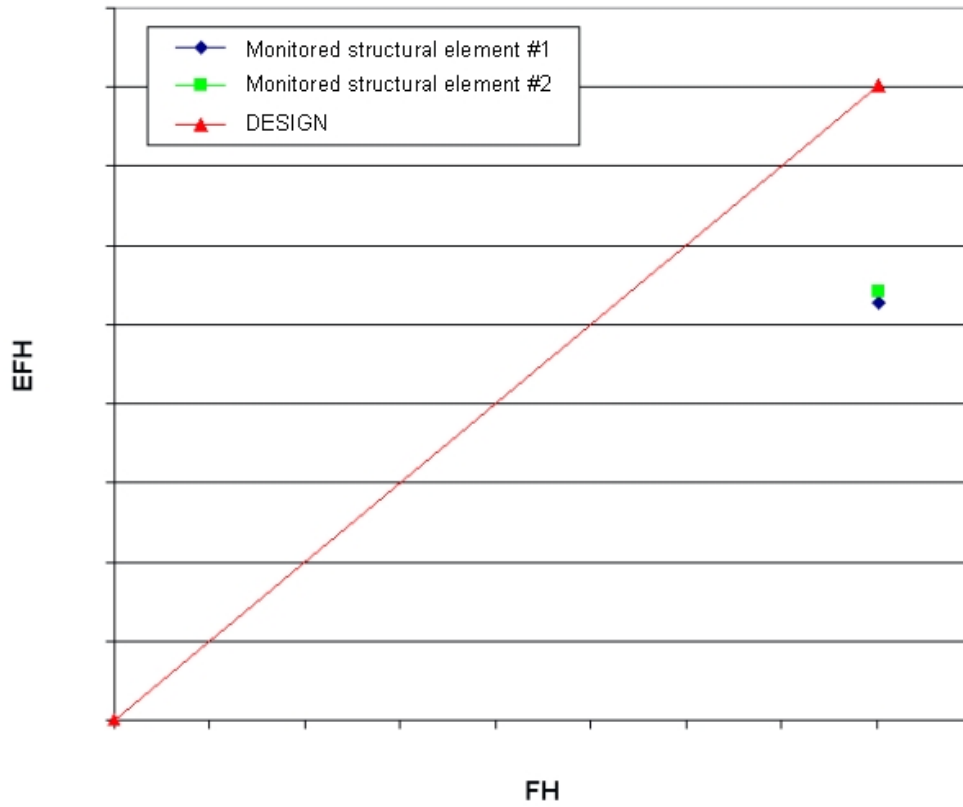


Fig. 7 - SF-260 Structural fatigue monitoring – comparison between flight hours and equivalent flight hours

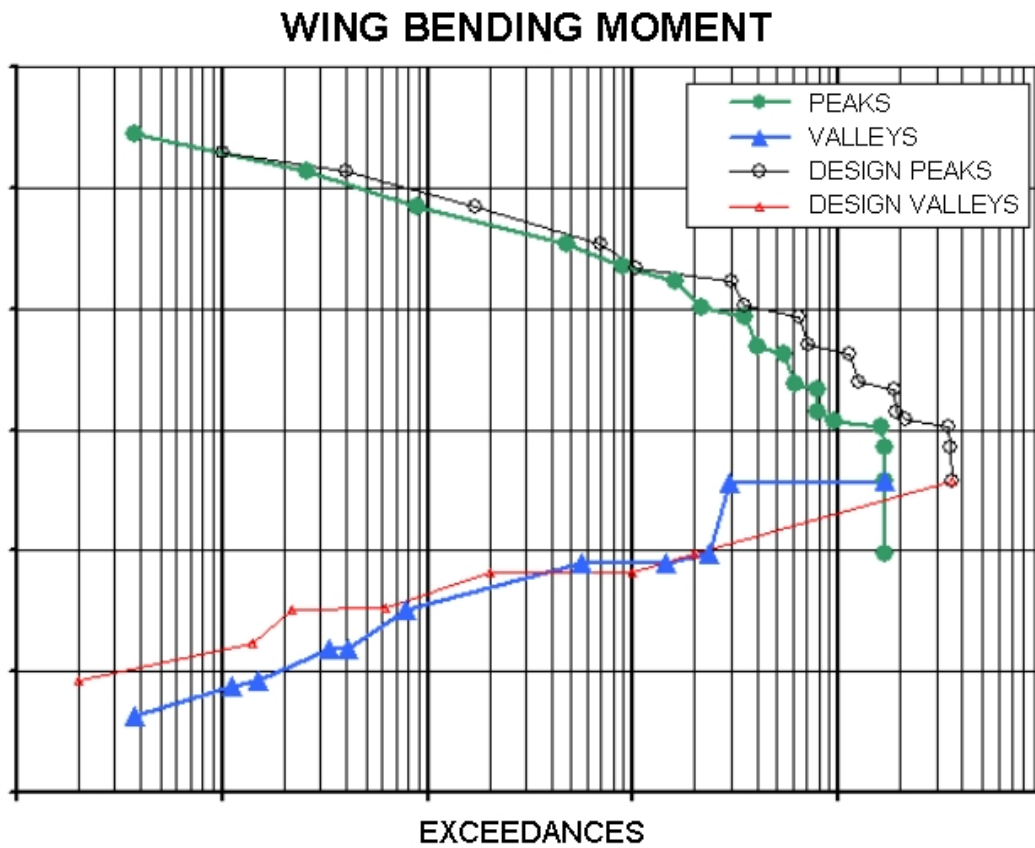


Fig. 8 - SF-260 Structural fatigue monitoring – comparison between recorded in-flight and fatigue test bending moment spectrum

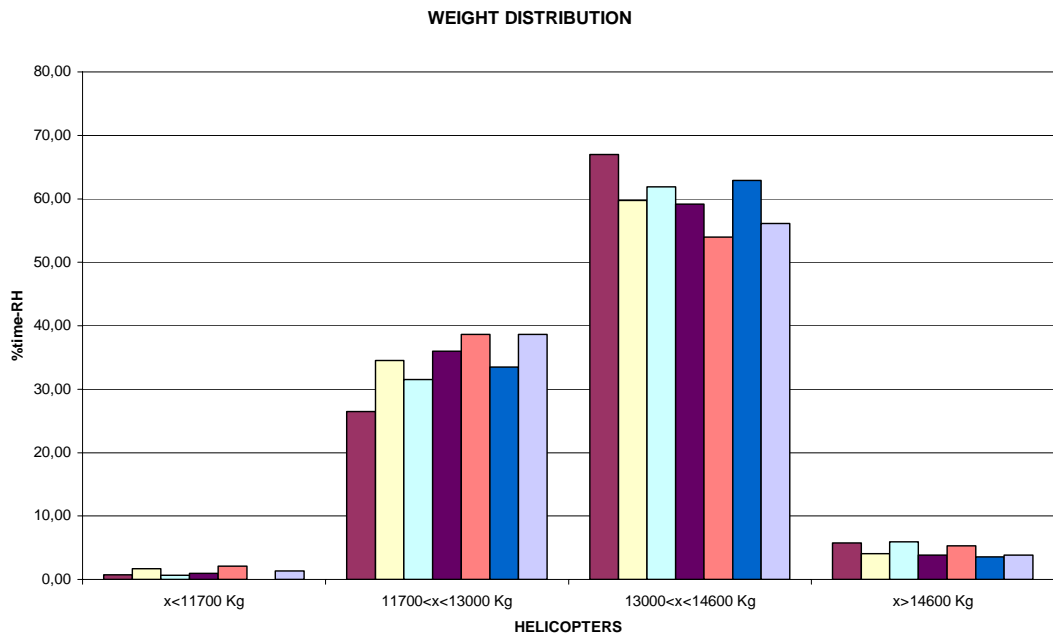


Fig. 9 - Weight distribution of the monitored machines of the Danish AW101 fleet.

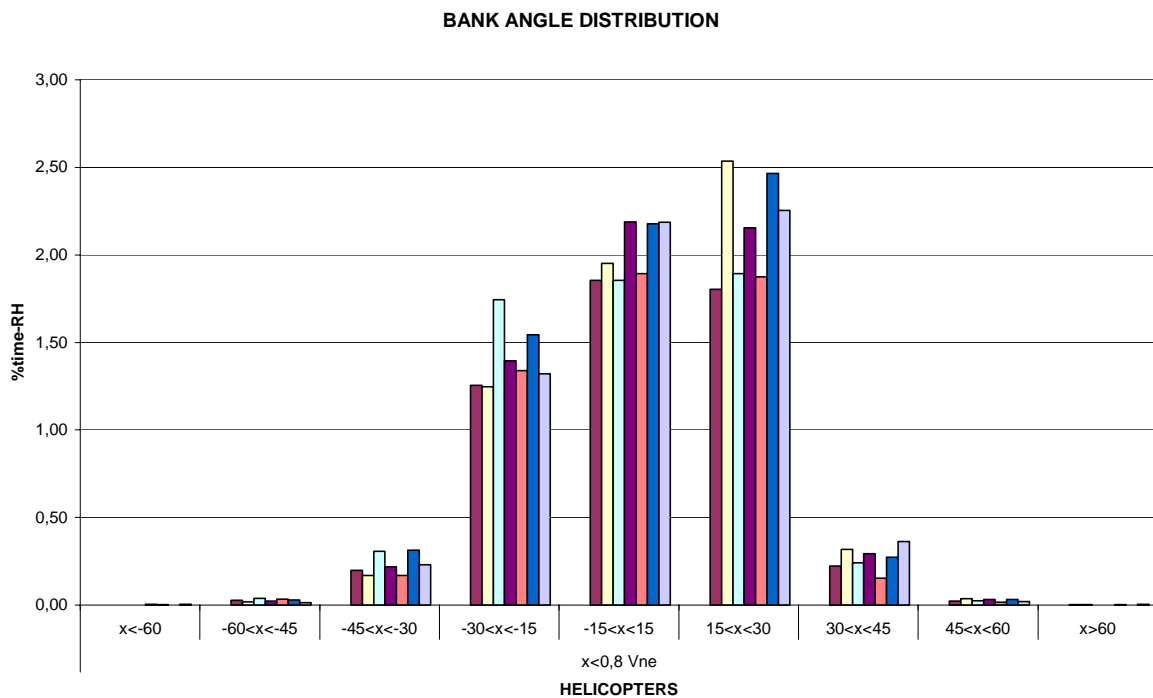


Fig. 10 - Bank angle distribution of the monitored machines of the Danish AW101 fleet.

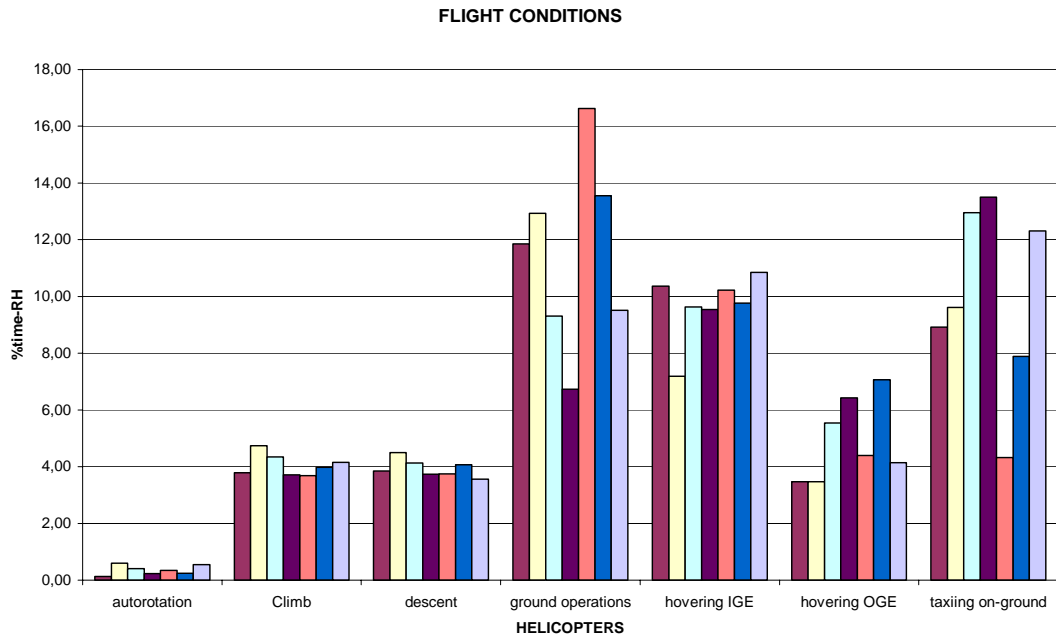


Fig. 11 - Distribution of some typical maneuvers of the monitored machines of the Danish AW101 fleet.

```

ALN I.A.T.P. VSN 3.0.0

C-27J NC      FLIGHT 337 Date: 2008/05/29
Start Time: 07:03:02
Sortie Time:  1.50 hr
Flight Time:  1.01 hr
Wgross/Xcg at Take-off: 25525. kg, 0.2856 mac
Wfuel      at Take-off:  5001. kg
Wpayload   at Take-off:   0. kg
Nr. Lift-offs:      2
Airdrop Events:    0

Processing Type:      Monitored

Total Flight Hours Cumulated:      430.42
Total Nr.of Flights Cumulated:     337
Total Flight Hours Treated As Unmonitored: 30.01
Total Nr.of Flights Treated As Unmonitored: 22

Control location      Actual Damage      LSif      LSiftot      LSIh      LSIhtot      RLftot      RLhtot
Wing upper panel:    0.2446E-02      1.194330      1.154710      2.000740      1.536796      13582.9      24338.5
Wing lower panel:    0.7828E-02      1.023553      0.794937      1.714641      1.057969      13704.1      24544.6
Wing root:           0.8401E-02      0.538655      0.447075      0.902441      0.595066      13821.3      24743.9
Horizontal tail root: 0.4731E-03      0.596827      0.642832      0.999670      0.855427      13755.4      24631.8
Vertical tail panel: 0.8049E-04      0.600104      1.113496      1.005202      1.481809      13596.8      24362.2
Crew door:           0.4548E-03      2.979498      1.966918      4.992308      2.618313      13309.1      23873.0
Ramp door:           0.3669E-03      3.076688      2.083430      5.153765      2.772663      13269.9      23806.6
Wing-nacelle attachment: 0.2199E-05      3.911610      3.417079      6.538969      4.538222      12820.4      23046.7
Main landing gear:   0.6477E-03      1.186286      0.845194      1.986929      1.124674      13687.2      24515.9

Control location      A-actual (mm)      ARL(hr)      A-design (mm)      DRL (hr)      A-detect (mm)      A-critic (mm)
Wing upper panel:    1.301211      34932.0      1.033945      37921.6      9.000      90.000
Wing lower panel:    1.032924      41257.9      1.066198      41041.6      10.000      118.810
Wing root:           1.290889      7306.8      1.407583      7197.6      20.470      20.000
Horizontal tail root: 1.016958      17089.7      1.075019      16756.6      8.900      13.000
Vertical tail panel: 1.020502      18854.4      1.344979      18449.6      50.000      76.000
Crew door:           1.056635      36794.4      1.030412      37165.6      5.400      53.940
Ramp door:           1.045299      19866.1      1.057872      19772.6      11.110      11.110
Wing-nacelle attachment: 1.000353      16486.8      1.003978      164214.6      2.500      18.000
Main landing gear:   1.111816      26929.0      1.213907      26723.6      15.000      40.000
    
```

Table I – Typical C27 J IATP output.

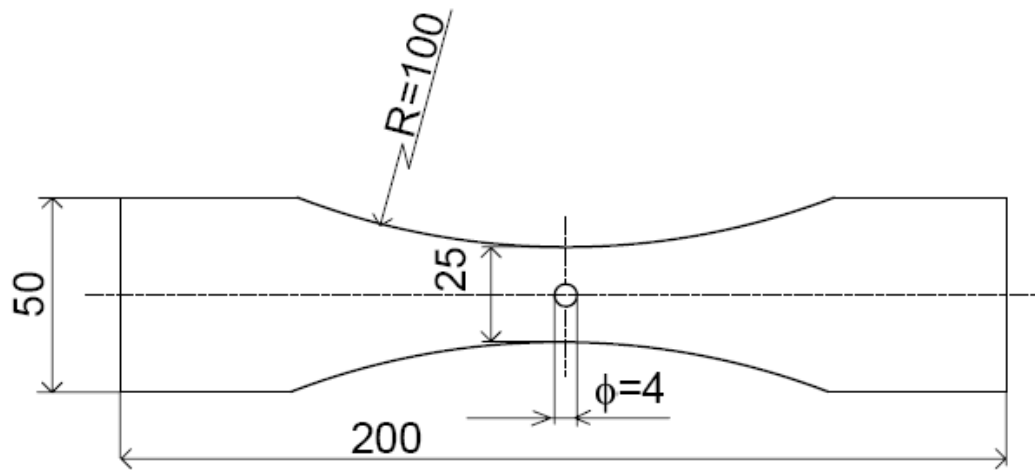


Fig. 12 - Open hole specimen.

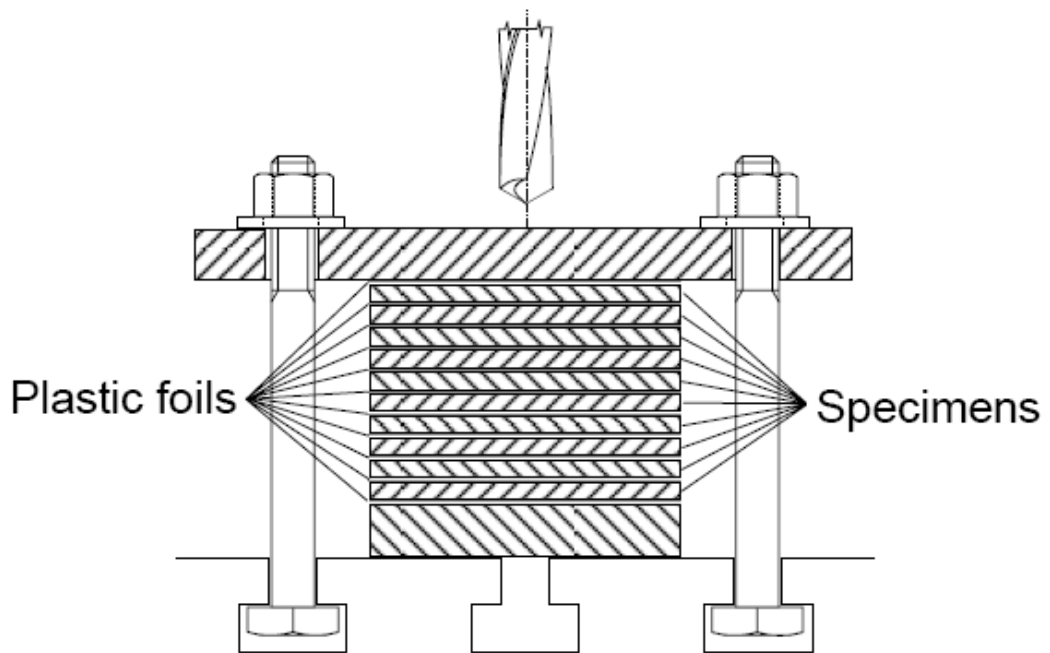


Fig. 13 - Machining Type B (without plastic foils) and Type C (with plastic foils) specimens.

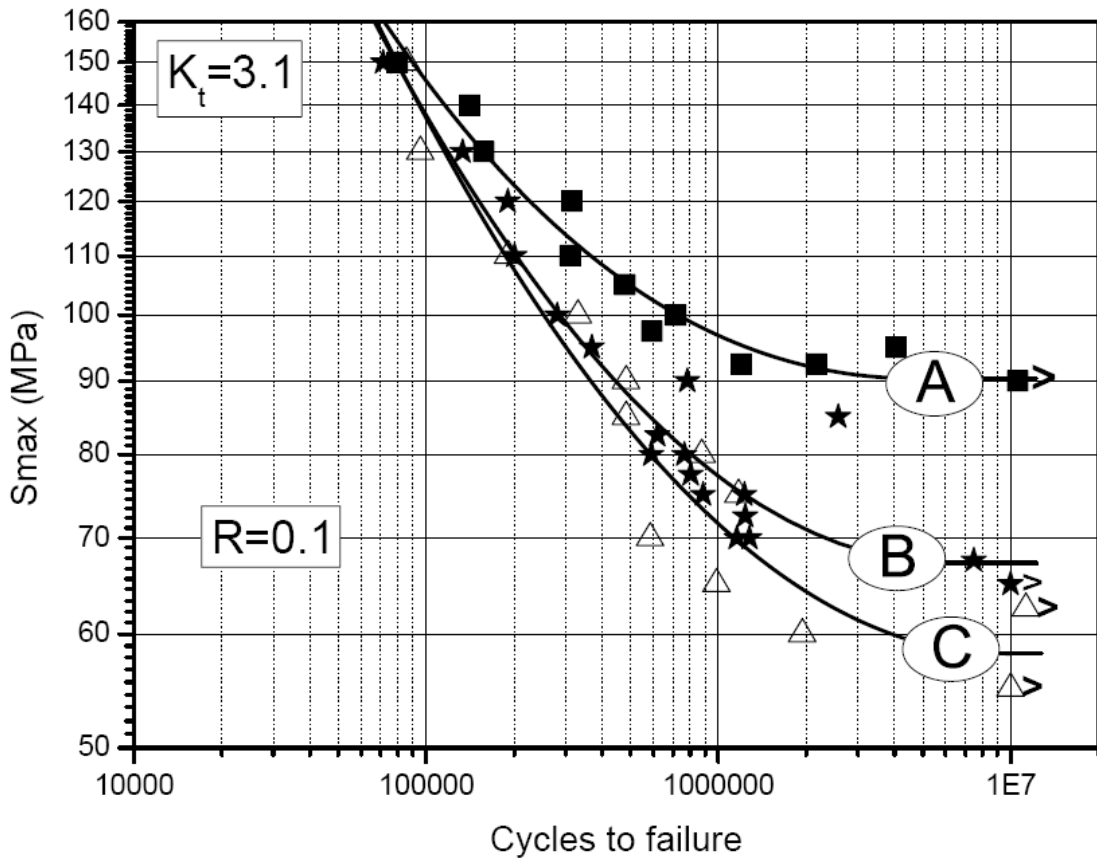


Fig. 14 - Fatigue test results of monolithic specimens.

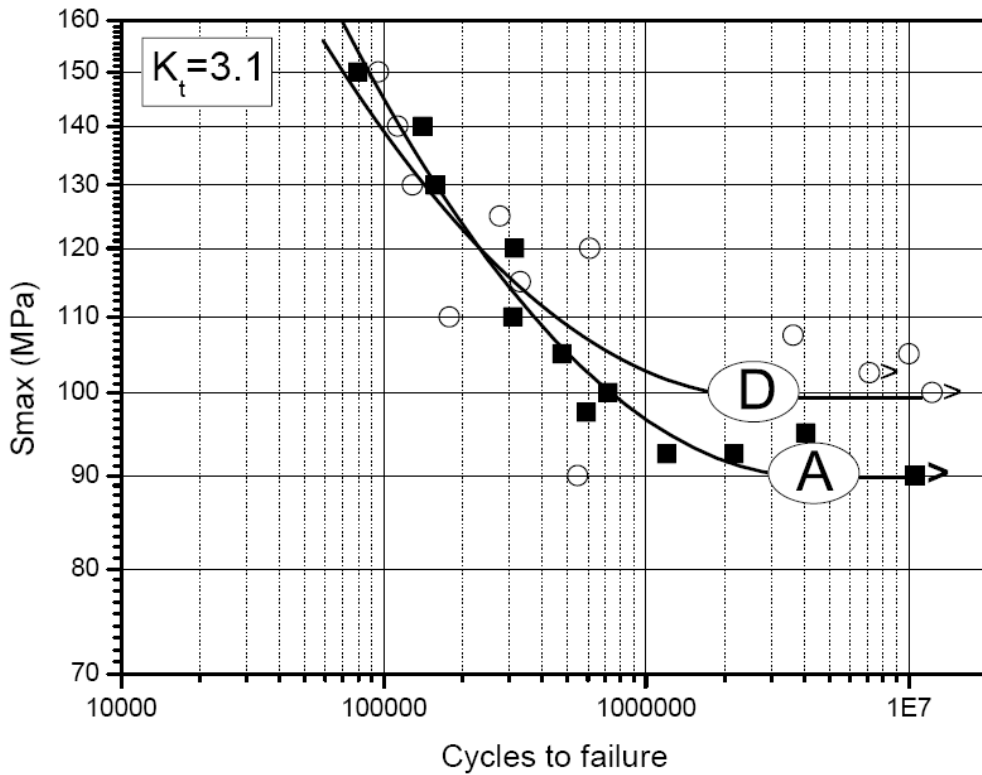


Fig. 15 - Fatigue test results of reference monolithic and metal laminated specimens.

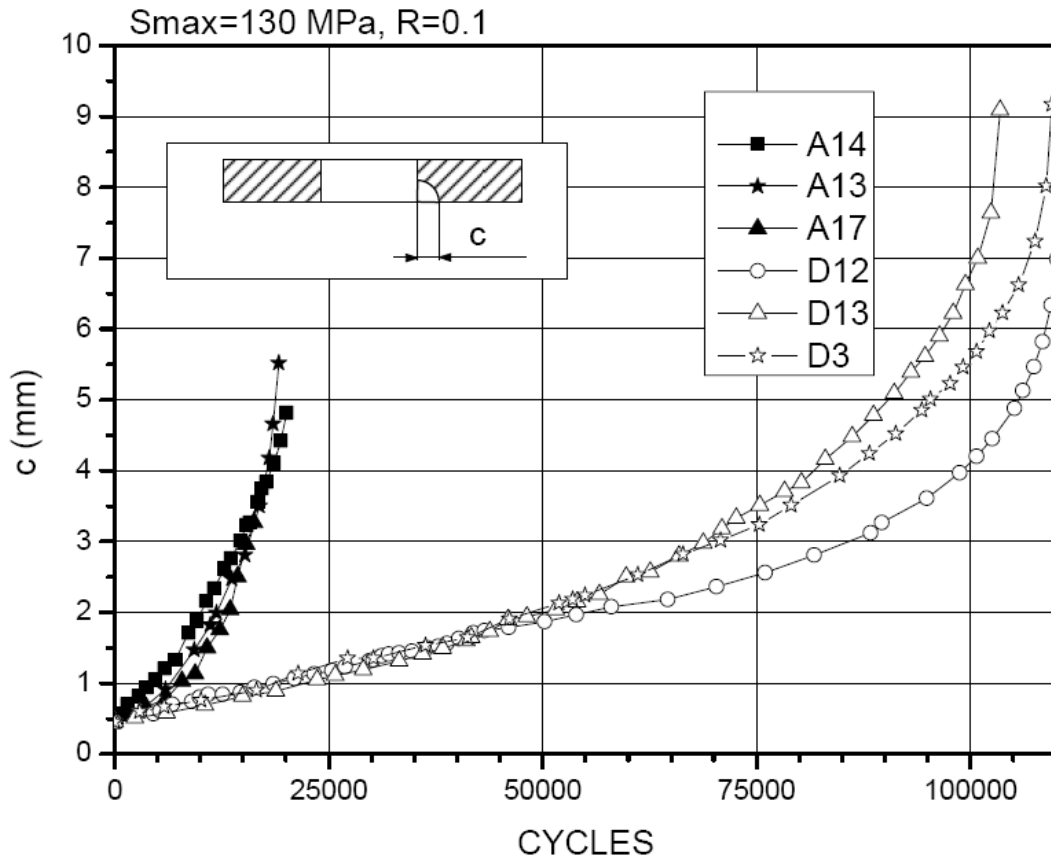


Fig. 16 - Crack propagation test results of monolithic and metal laminated specimens.

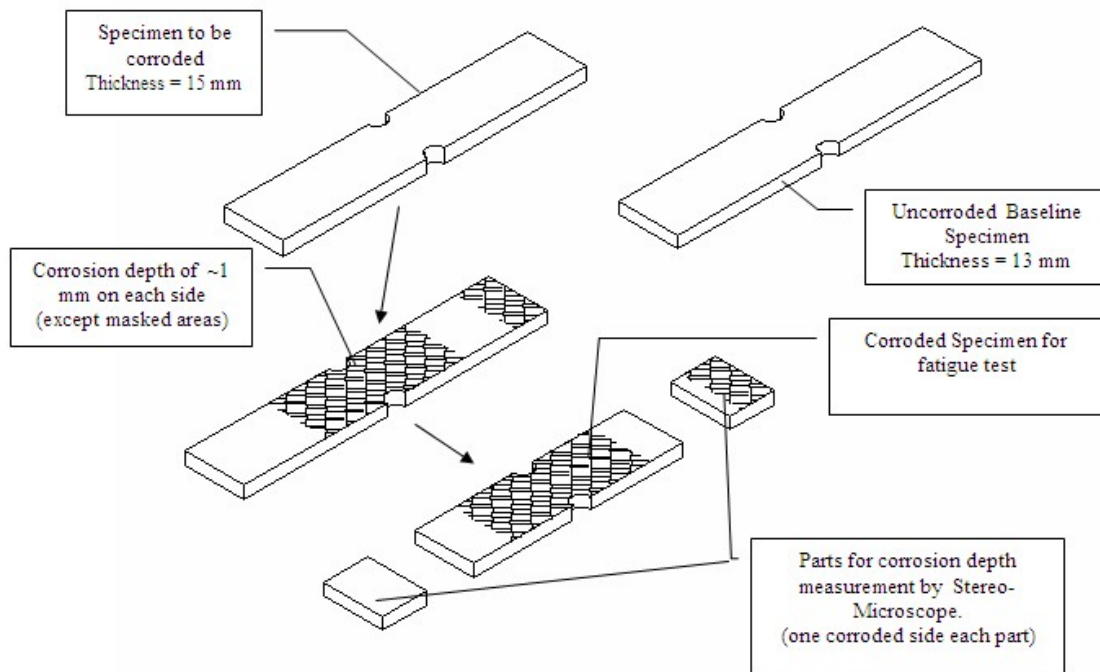


Fig. 17 - Differences in corroded and un-corroded side notched specimens.

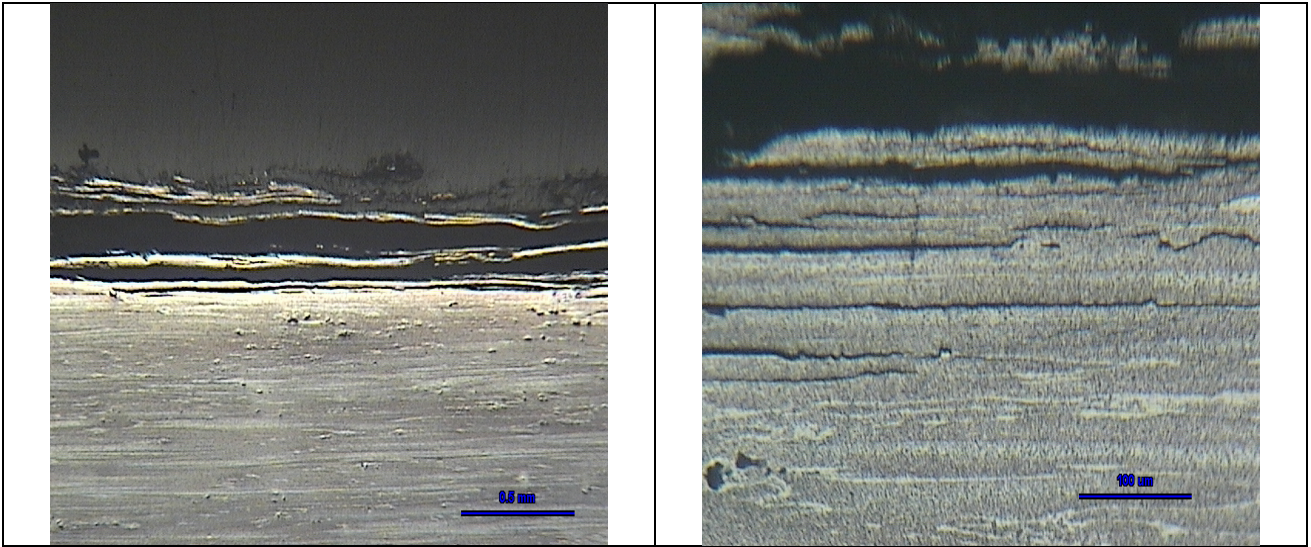


Fig. 18 – Micrographs (at 20X left, at 100X right) of corroded specimen.

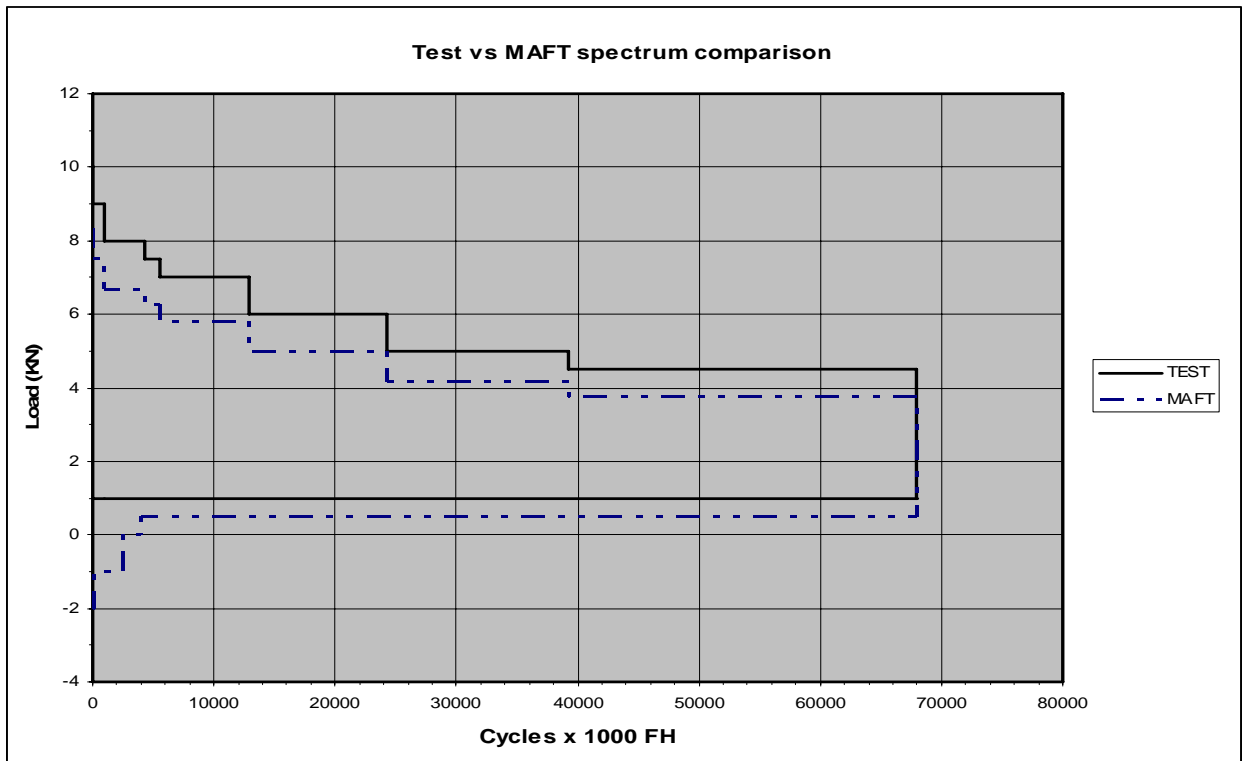


Fig. 19 - Modified Tornado fatigue spectrum for the corrosion-fatigue interaction investigation.

Test Group Number	Material	Manufacturing
451	VIM-VAR 9310	Ground fillet, shotpeened
551	VIM-VAR 9310	Unground fillet, shotpeened
651	VAR 9310	Ground fillet, shotpeened
751	VIM-VAR EX 53	Ground fillet, shotpeened

Table II - Four configurations of case carburized steel gears investigated.

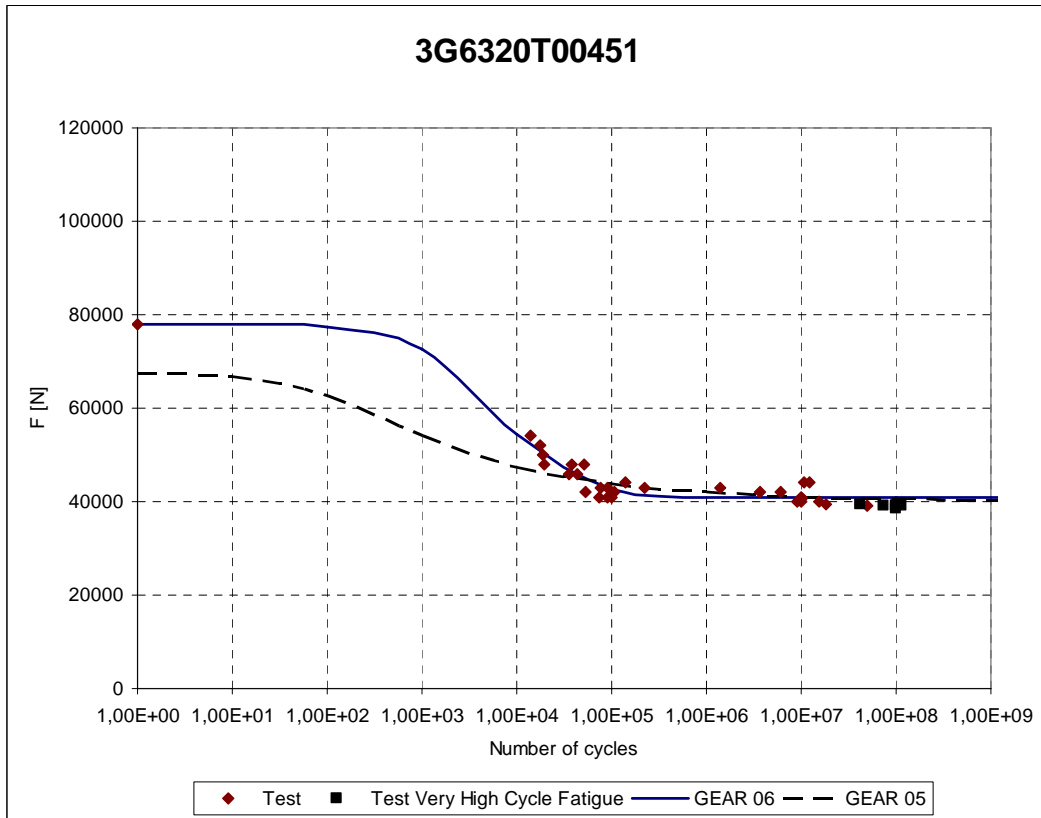


Fig. 20 - Analysis of fatigue results from carburized material, based on different shape curves.

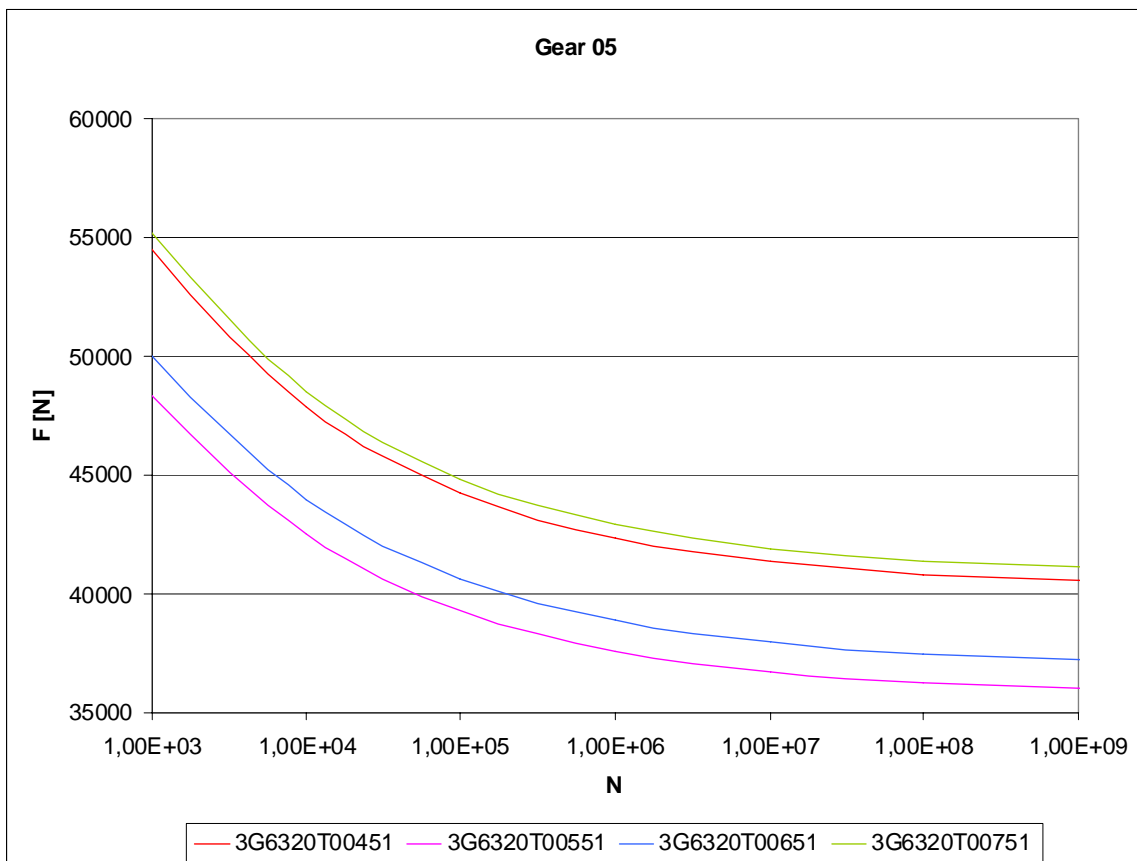


Fig. 21 - S-N curves of 4 case carburized steels for gear applications.

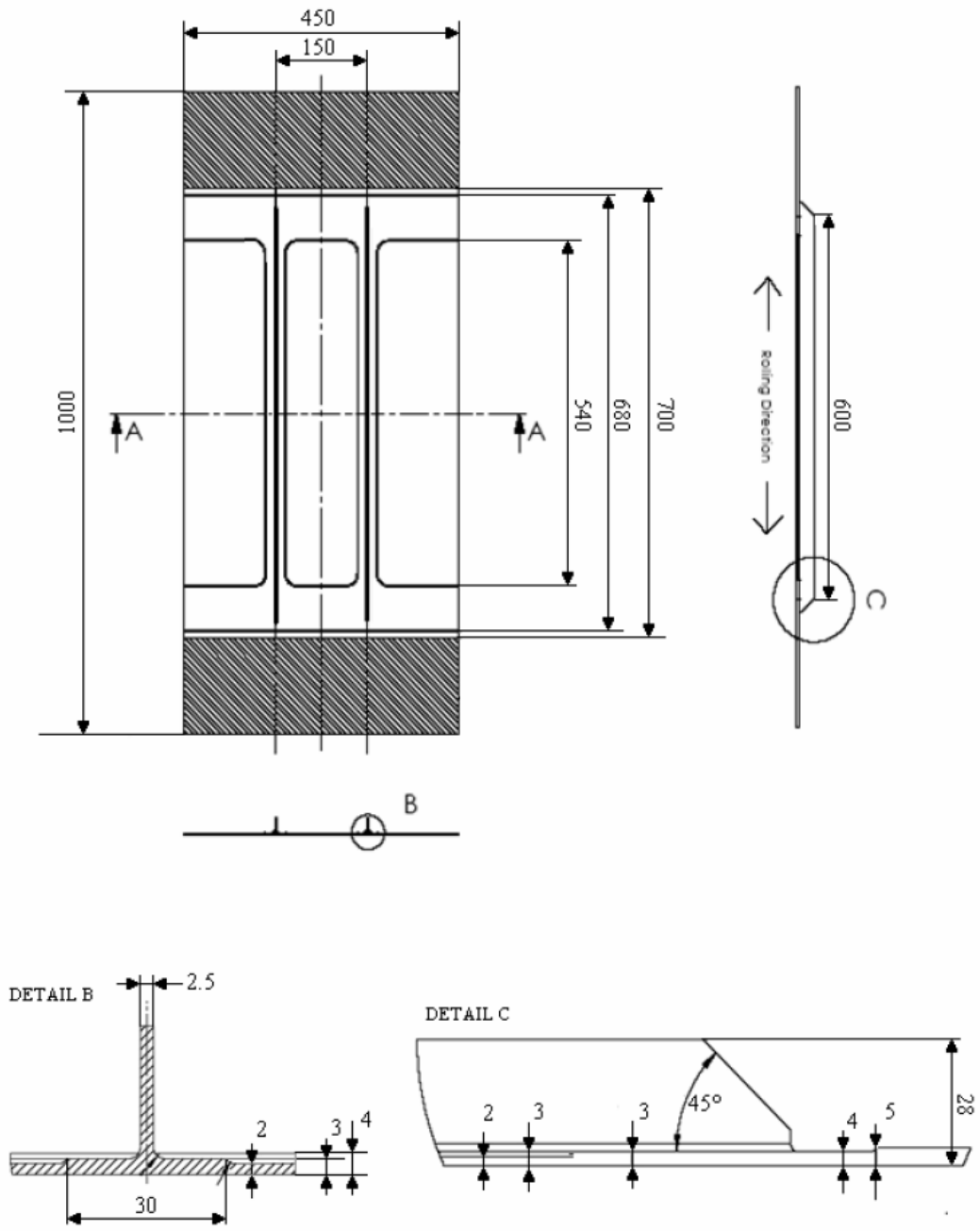


Fig. 22 - DaToN panel geometry.

Specimen		80 MPa, R = 0.1	110 MPa, R = 0.5
6056	HSM	1	1
	LBW1	1	1
	LBW1-PWHT	1	1
	LBW2	1	1
	LBW2-PWHT	1	1
	FSW	1	1
2024	LBW1	1	1
	LBW2	1	1

Table III – DaToN project: crack propagation test program performed in Pisa.

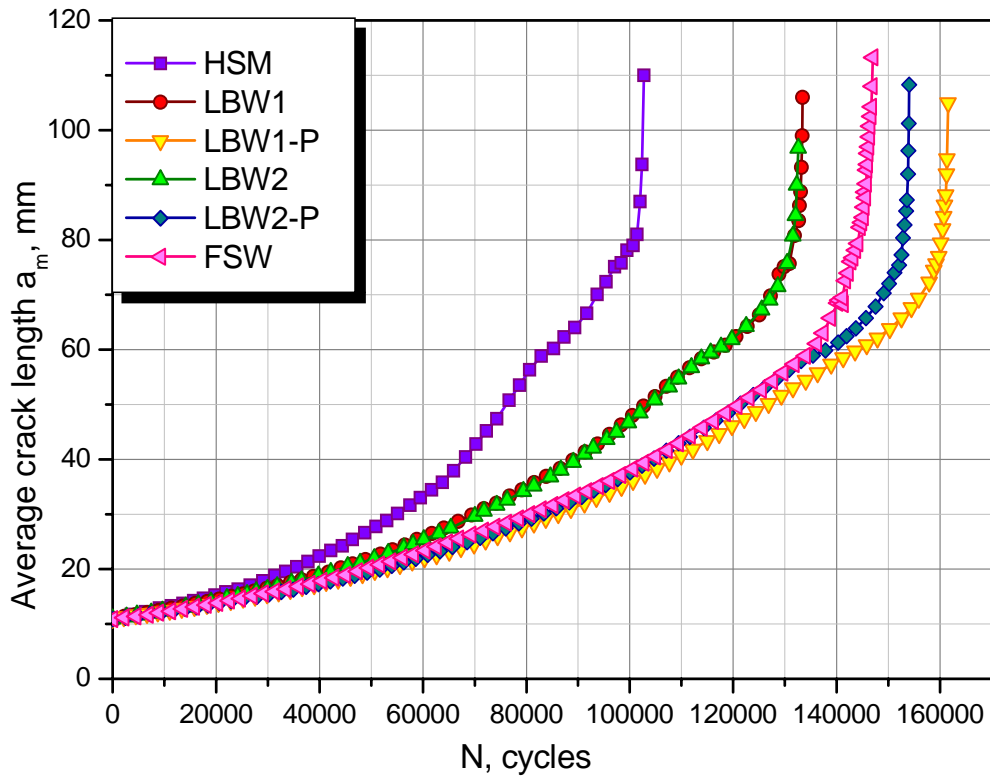


Fig. 23 – DaToN project: crack propagation in 6056 panels: 80 MPa, R=0.1 (tests performed in Pisa).

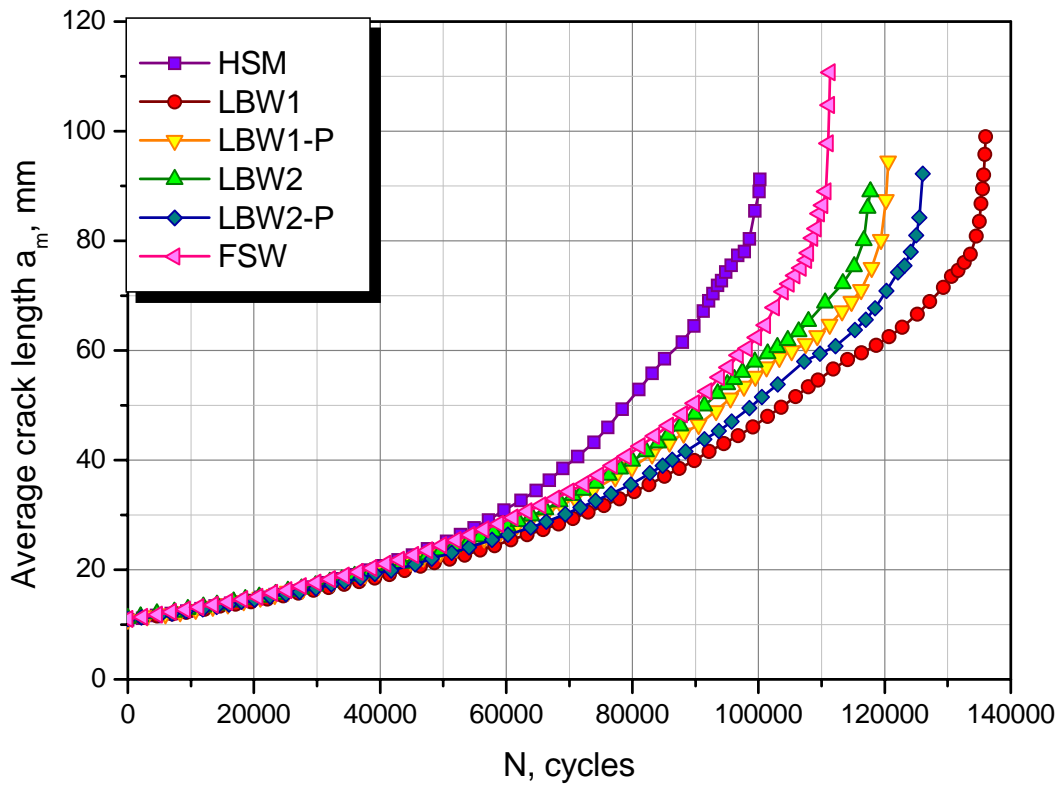


Fig. 24 – DaToN project: crack propagation in 6056 panels: 110 MPa, R=0.5 (tests performed in Pisa).

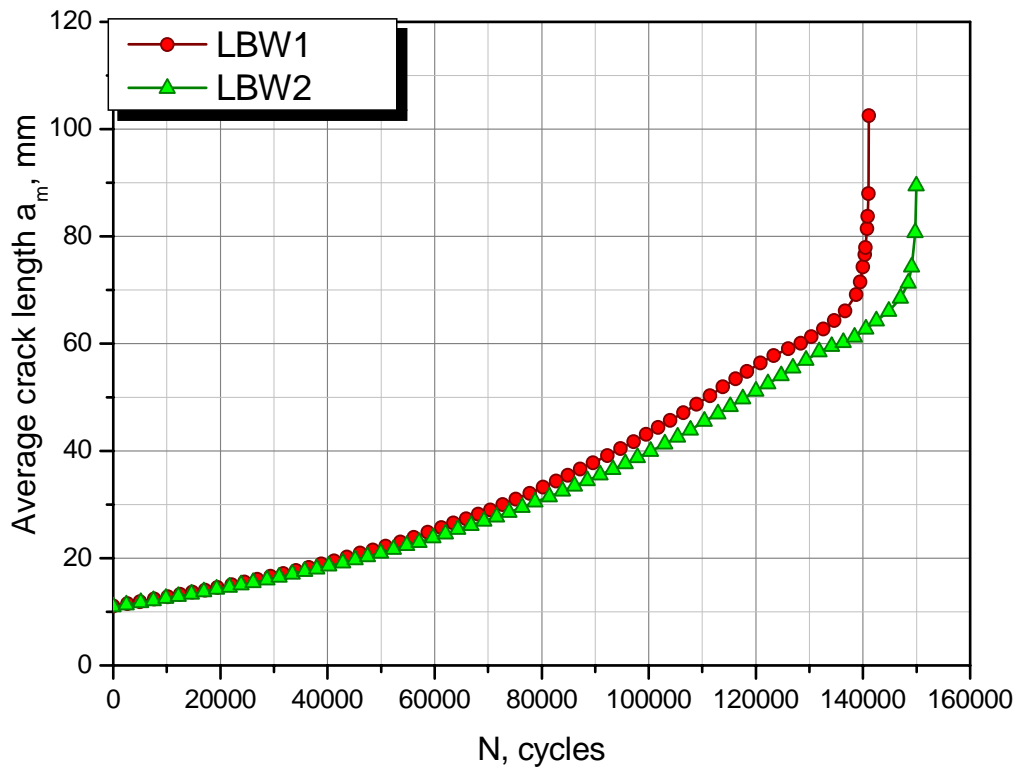


Fig. 25 – DaToN project: crack propagation in 2024 panels: 80 MPa, R=0.1 (tests performed in Pisa).

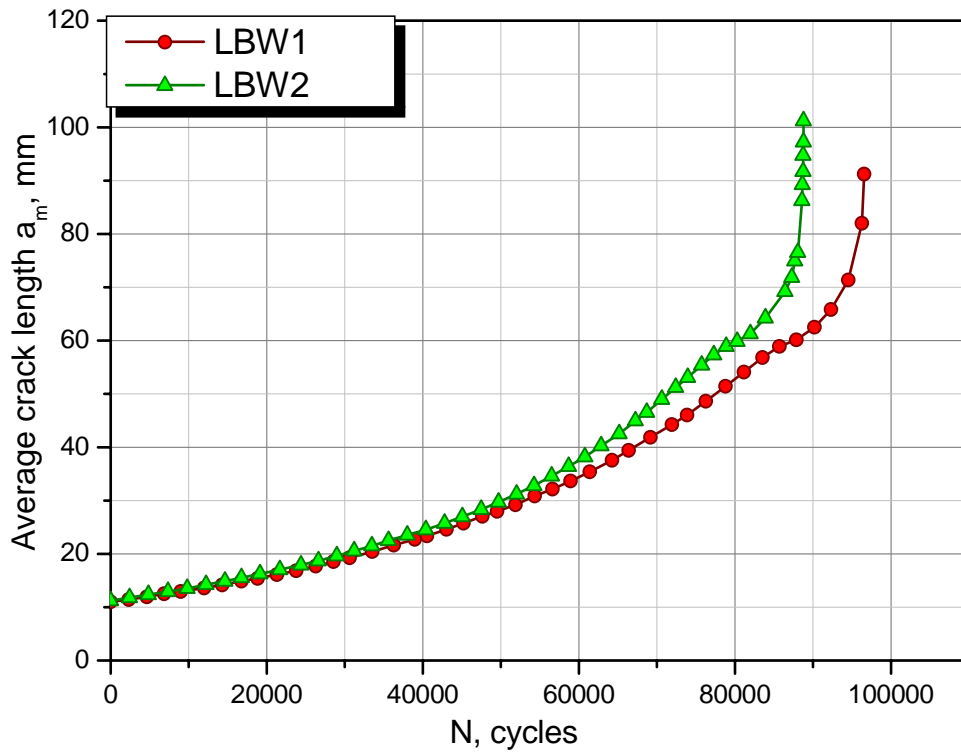


Fig. 26 – DaToN project: crack propagation in 2024 panels: 110 MPa, R=0.5 (tests performed in Pisa).

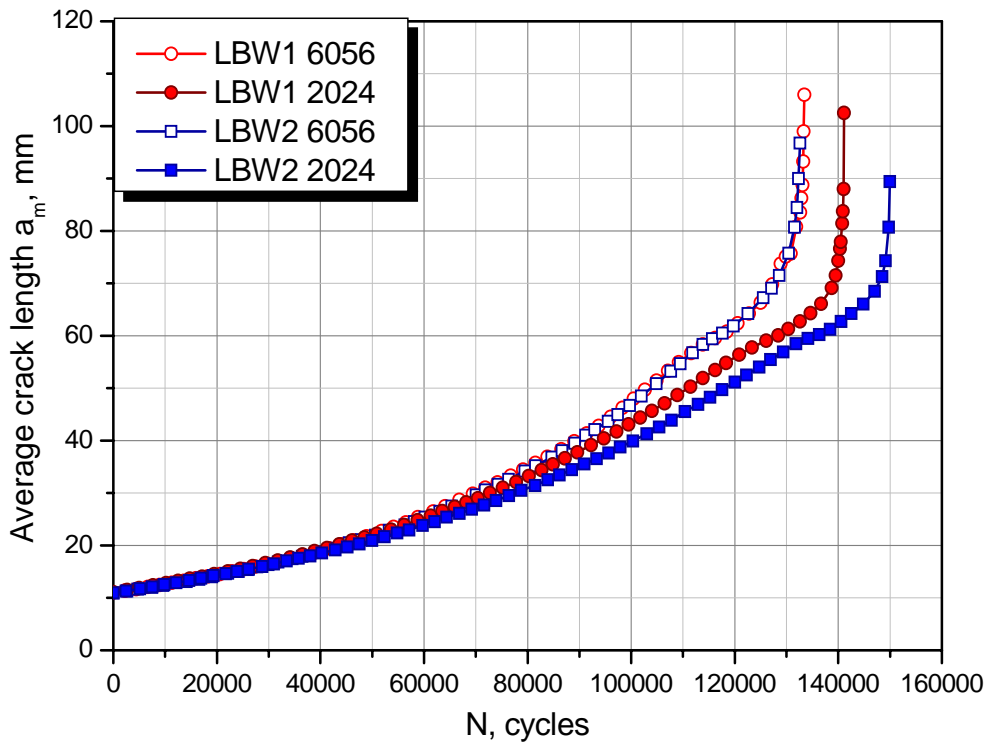


Fig. 27 – DaToN project: crack propagation in 6056 and 2024 panels at 80 MPa, R=0.1 (tests performed in Pisa).

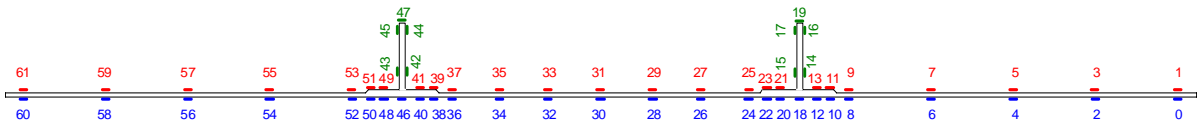


Fig. 28 – DaToN project: strain gauge map for residual stress measurement.

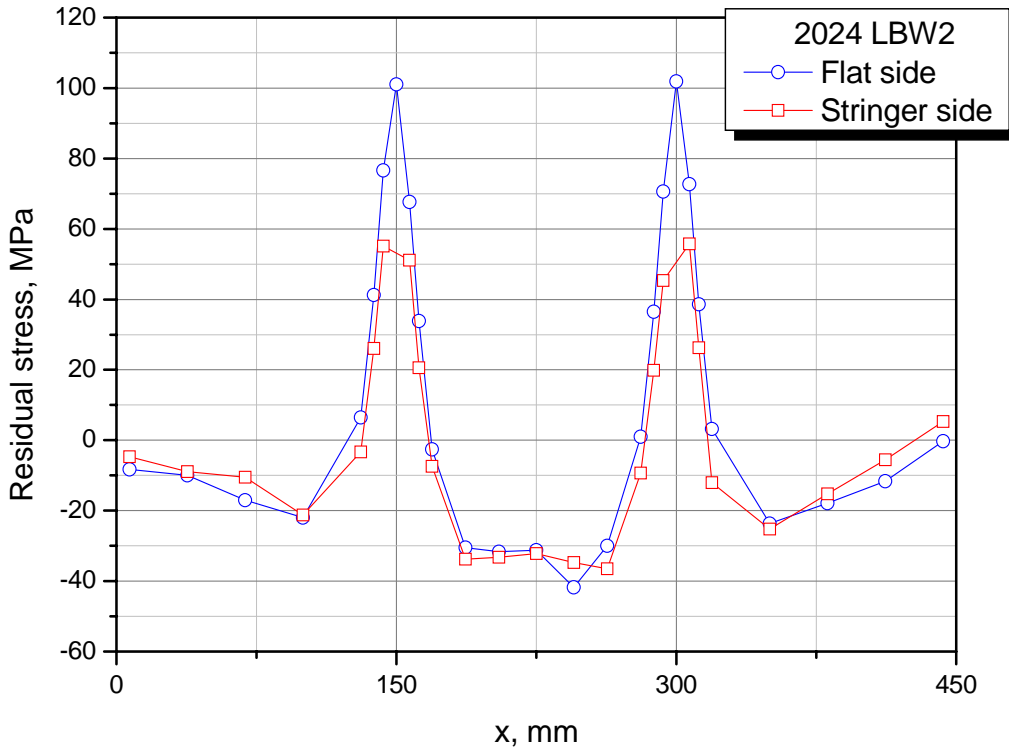


Fig. 29 – DaToN project: residual stresses in panel 2024 LBW2.

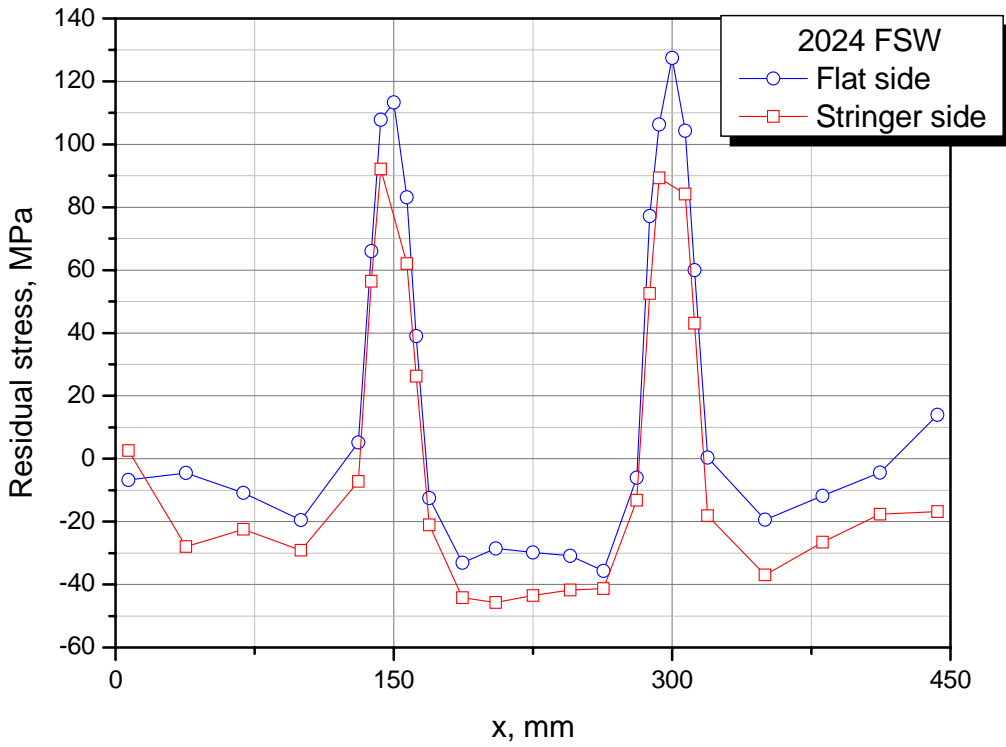


Fig. 30 – DaToN project: residual stresses in panel 2024 FSW.

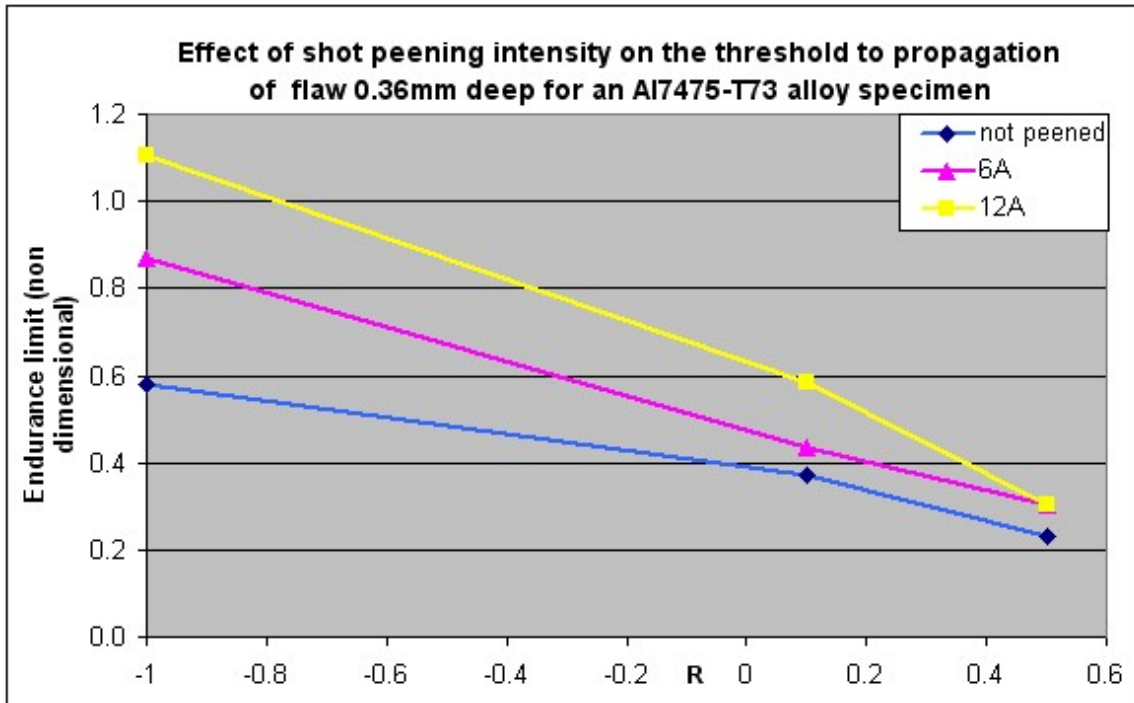


Fig. 31 - Effect of shot peening intensity on no-growth threshold for 7475-T73. Influence of stress ratio.

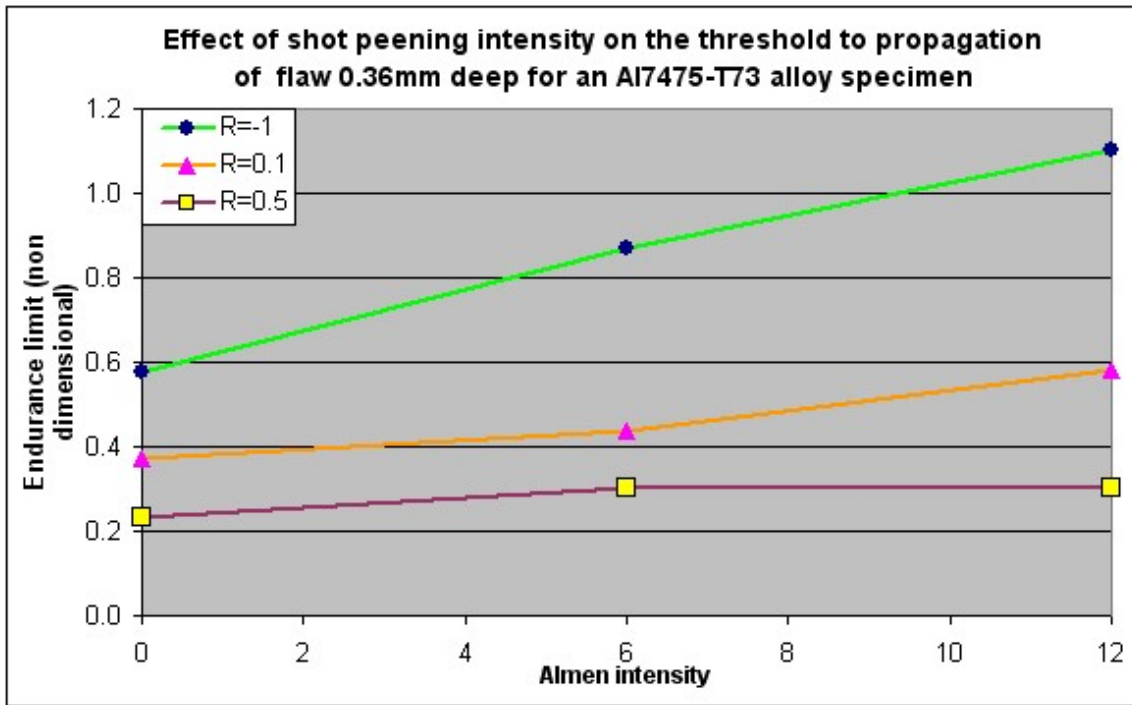


Fig. 32 - Effect of shot peening intensity on no-growth threshold for 7475-T73. Influence of Almen intensity.

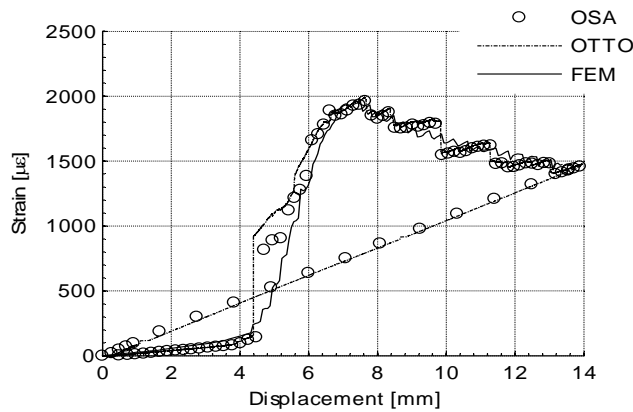


Fig. 33 - Strain measured (OSA and OTTO) and simulated (FEM) by the embedded sensor during the DCB test

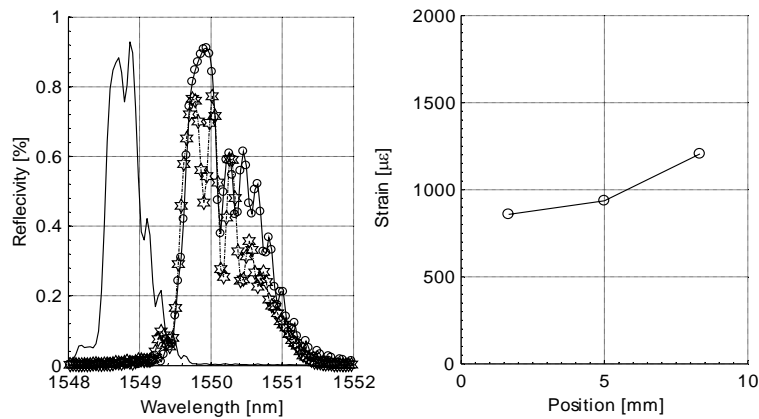


Fig. 34 - Spectrum acquired (circle) and simulated (stars) with strain distribution along FBG associated.

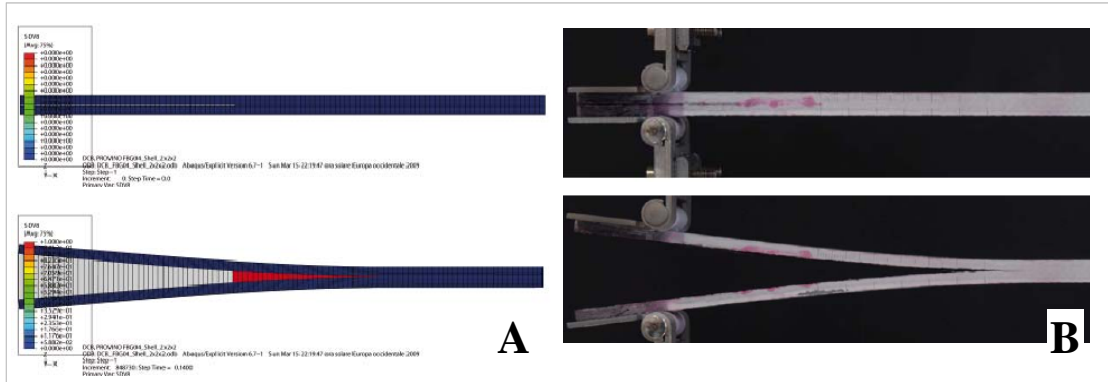


Fig. 35 - Numerical (A) and experimental (B) steps of a DCB test.

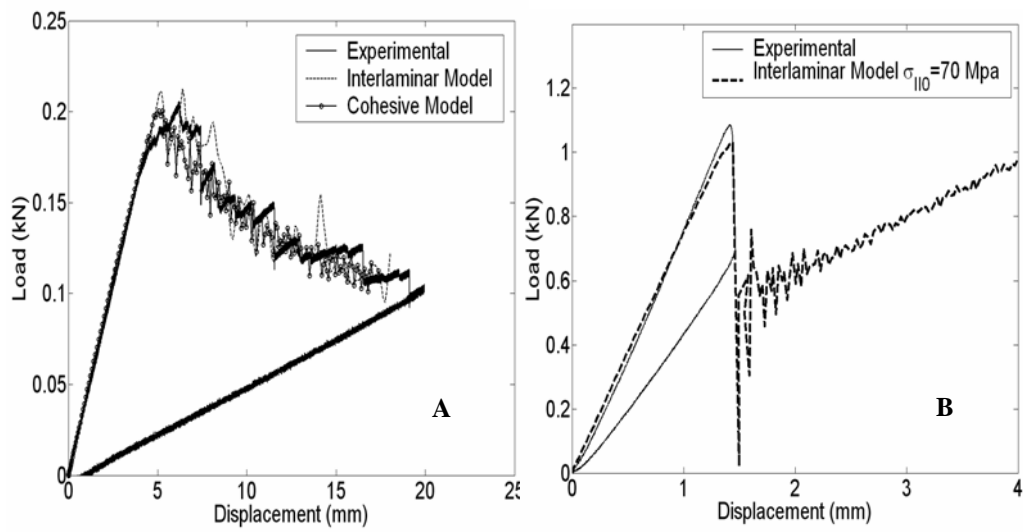


Fig. 36 - Numerical-experimental correlation of DCB FB test (A); and ENF UD test (B).

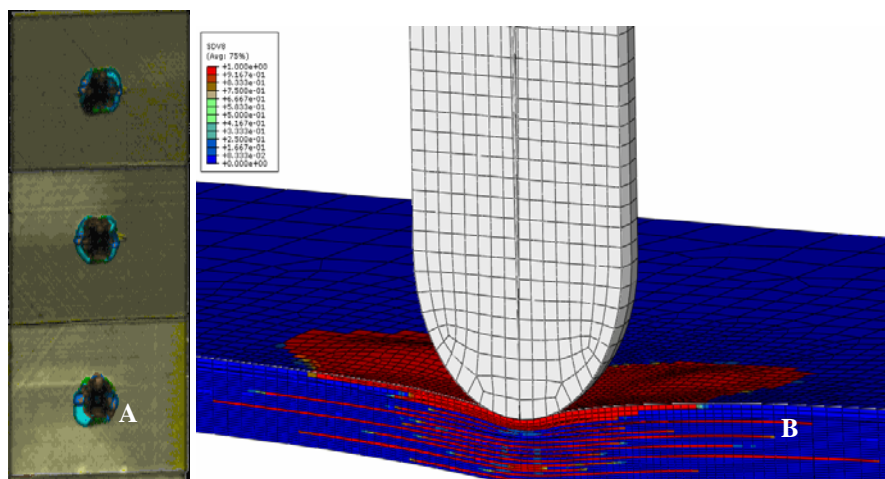


Fig. 37 - C-Scan results (A) and analysis (B) of a 20 J impact.



Fig. 38 - Out-of-plane deformation of defective composite stiffened panel under uniaxial compression.

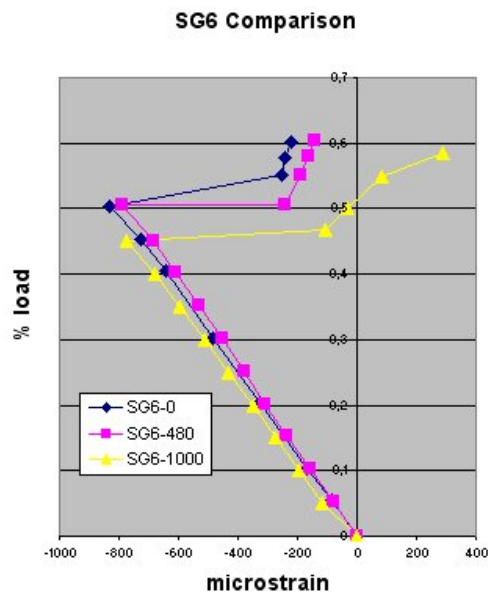


Fig. 39 - Strain gauge measurements in the damage location at different number of cycles.

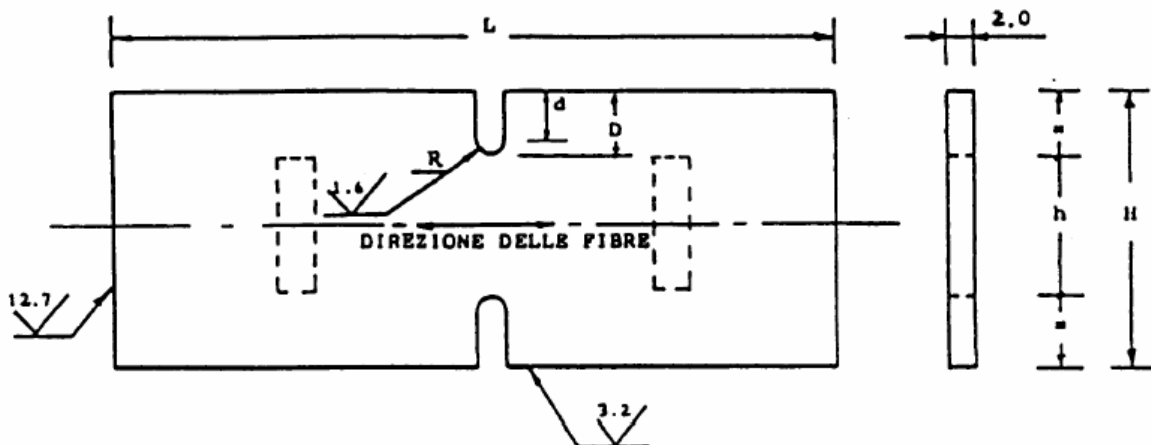


Fig. 40 - Typical OAST-OASB fatigue tests coupon.

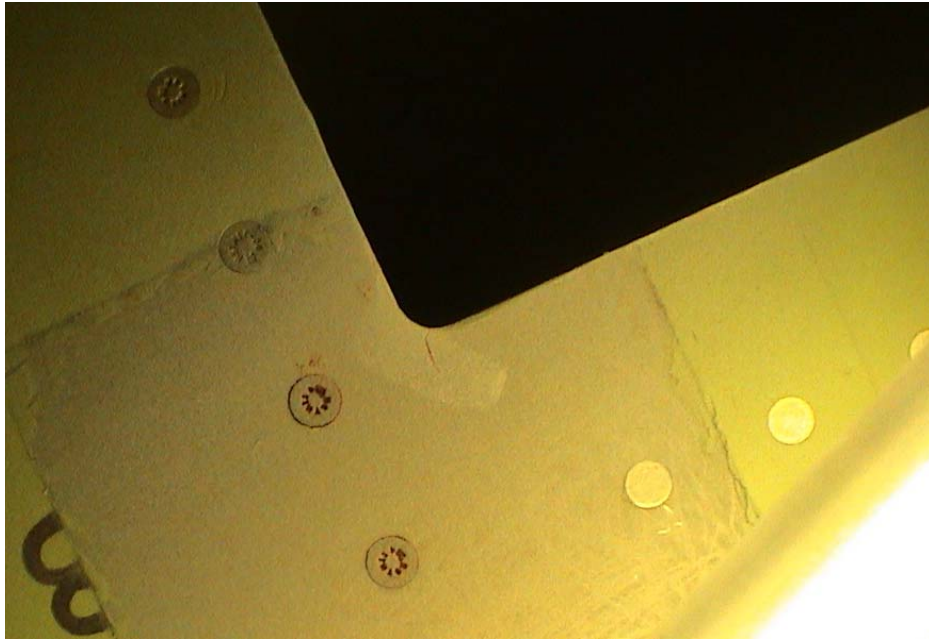


Fig. 41 - M-346 LH Prototype Wing development fatigue test – crack at the lower skin radius between flap and aileron

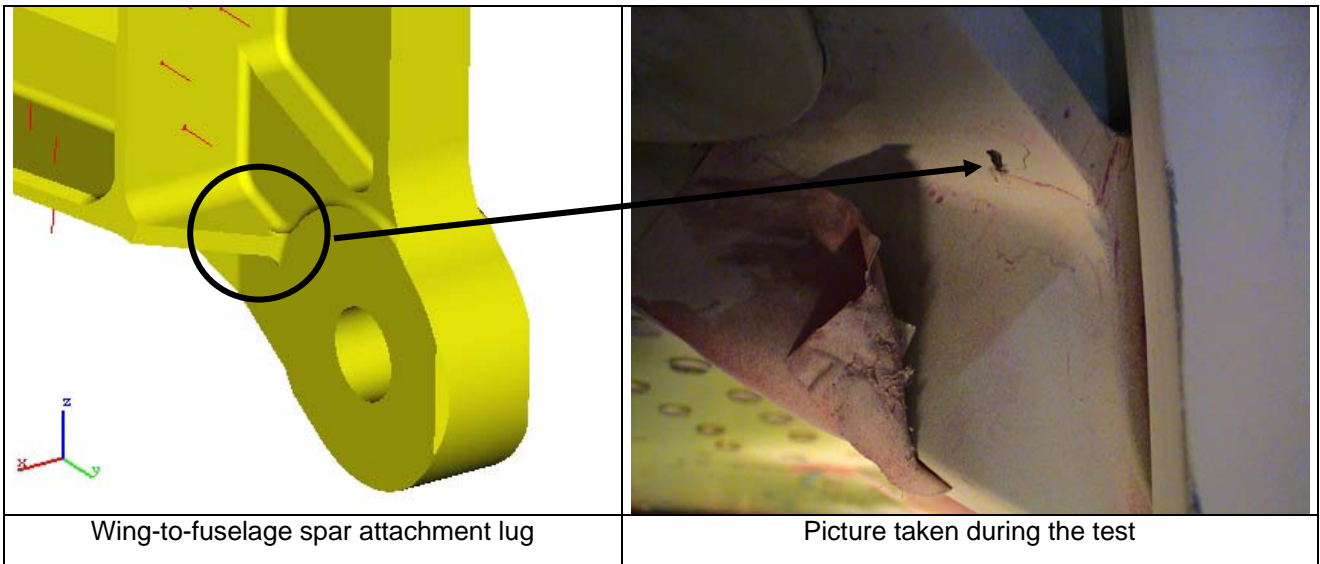


Fig. 42 - M-346 LH Prototype Wing development fatigue test – crack at spar root section

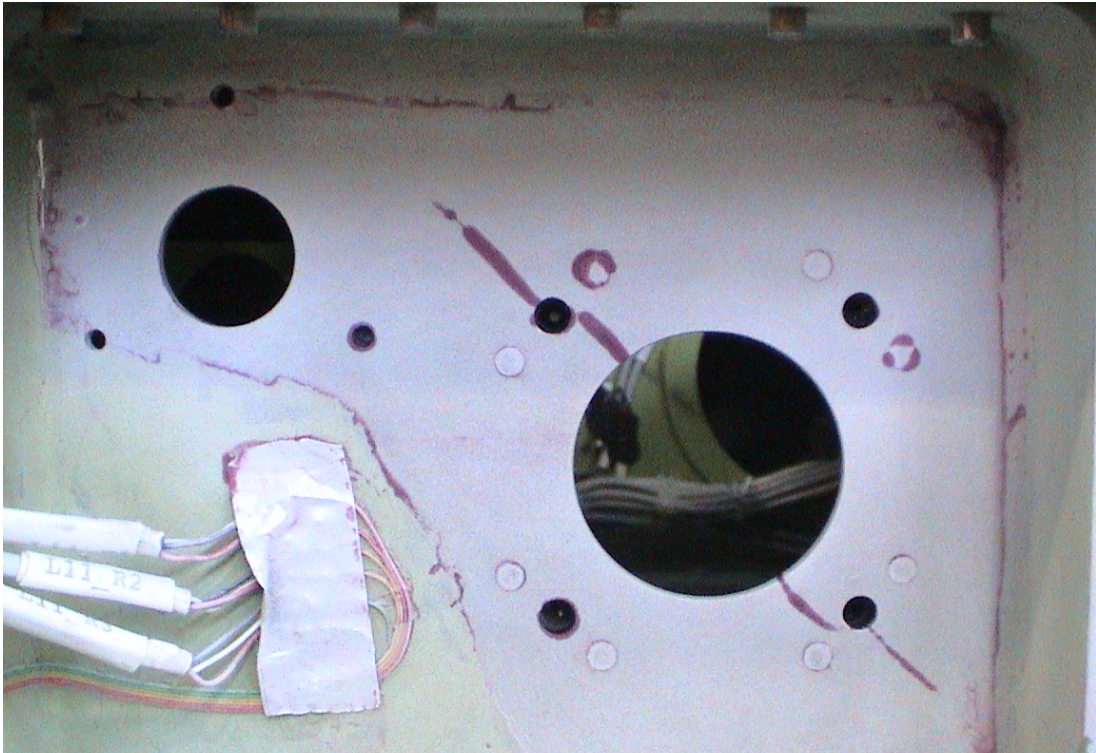


Fig. 43 - M-346 LH Prototype Wing development fatigue test – crack at circular web hole of front spar

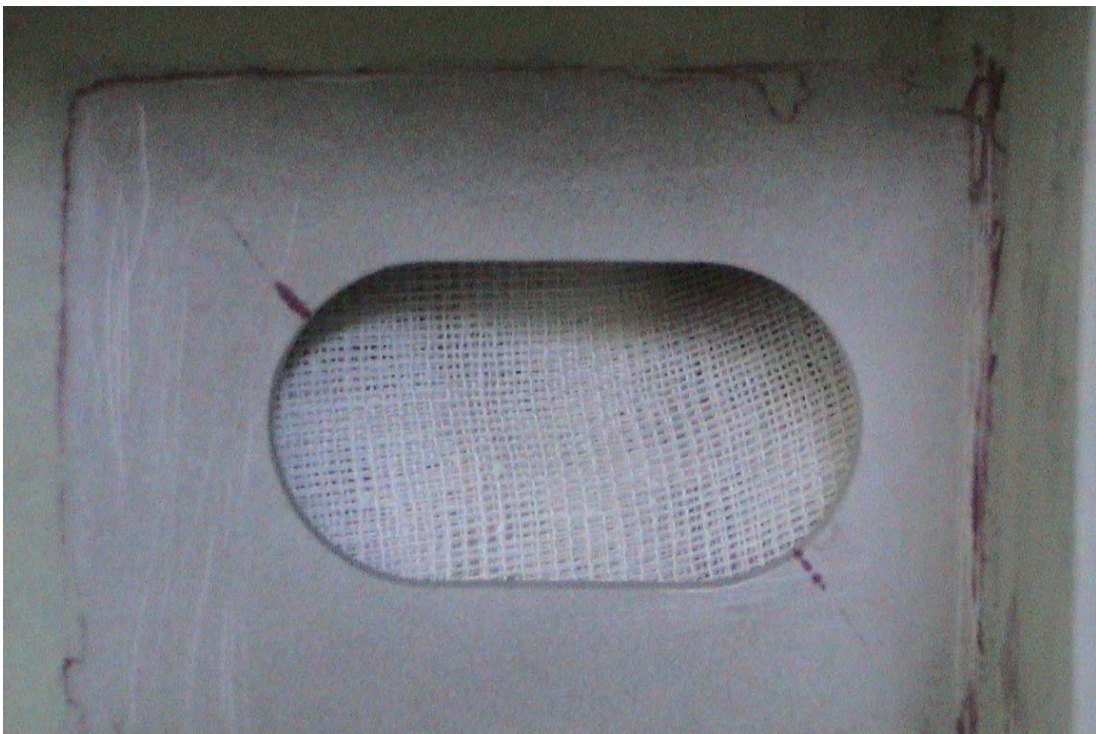


Fig. 44 - M-346 LH Prototype Wing development fatigue test – crack at rectangular web hole with round corners of front spar

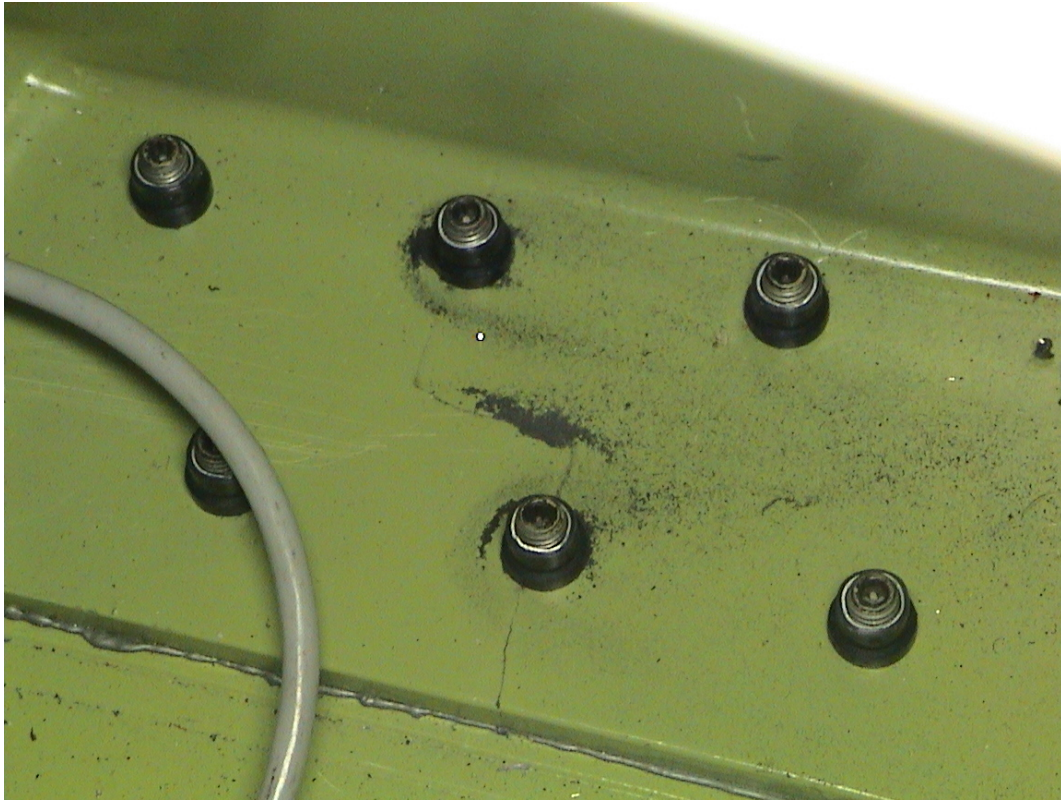


Fig. 45 - M-346 LH Prototype Wing development fatigue test – crack at lower cap of the first main spar

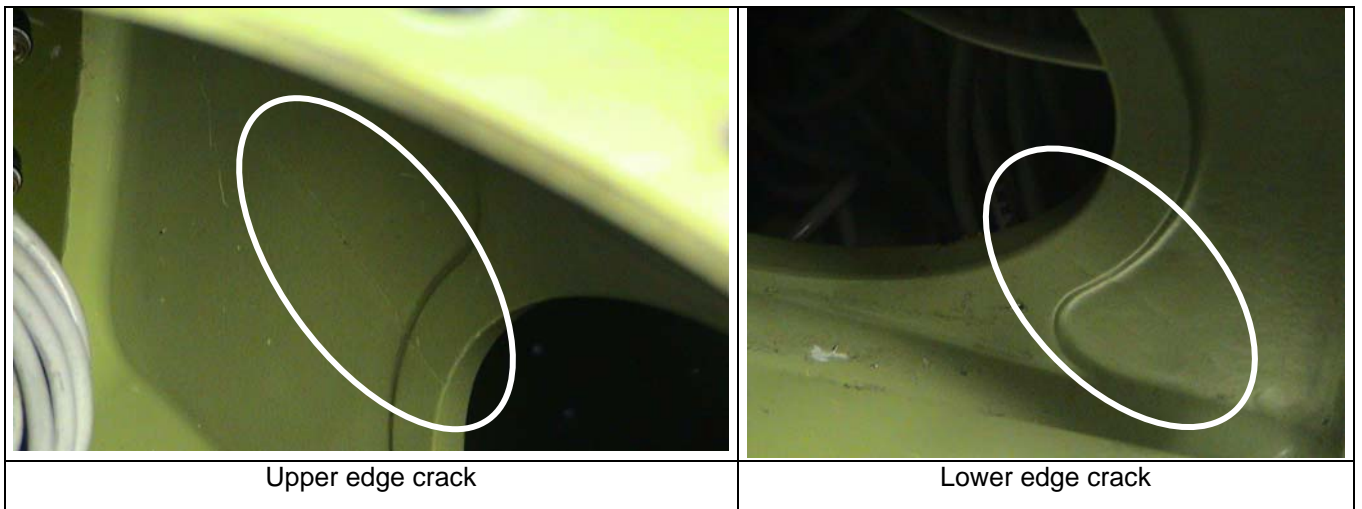


Fig. 46 - M-346 LH Prototype Wing development fatigue test – crack at elliptical web hole of the first main spar



Fig. 47 - M-346 LH Prototype Wing development fatigue test – crack on the spar cap carrying the flap attachments



Fig. 48 - Detail of B.787 Horizontal Tail composite structure in the fatigue test. (Half structure was tested).



Fig. 49 – B. 787 Horizontal Tail test rig.
(The complete structure was tested, to qualify the metallic parts).



Fig. 50 - RRJ Superjet 100.

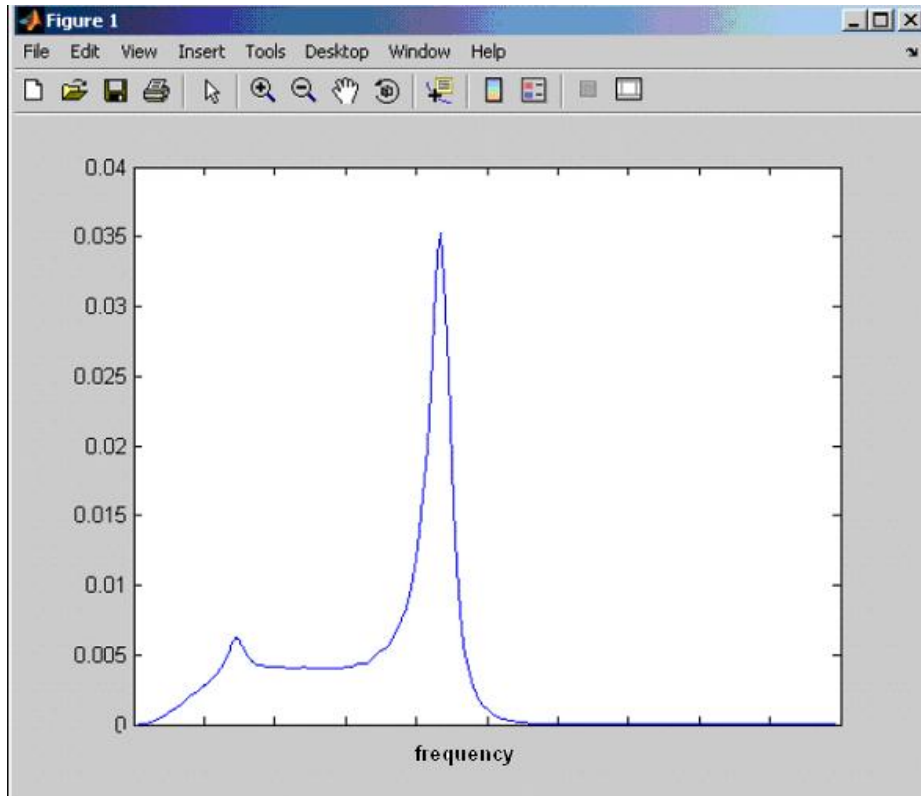


Fig. 51 - M-346 Analytical methodologies development – example of PSD generation for buffet analysis.

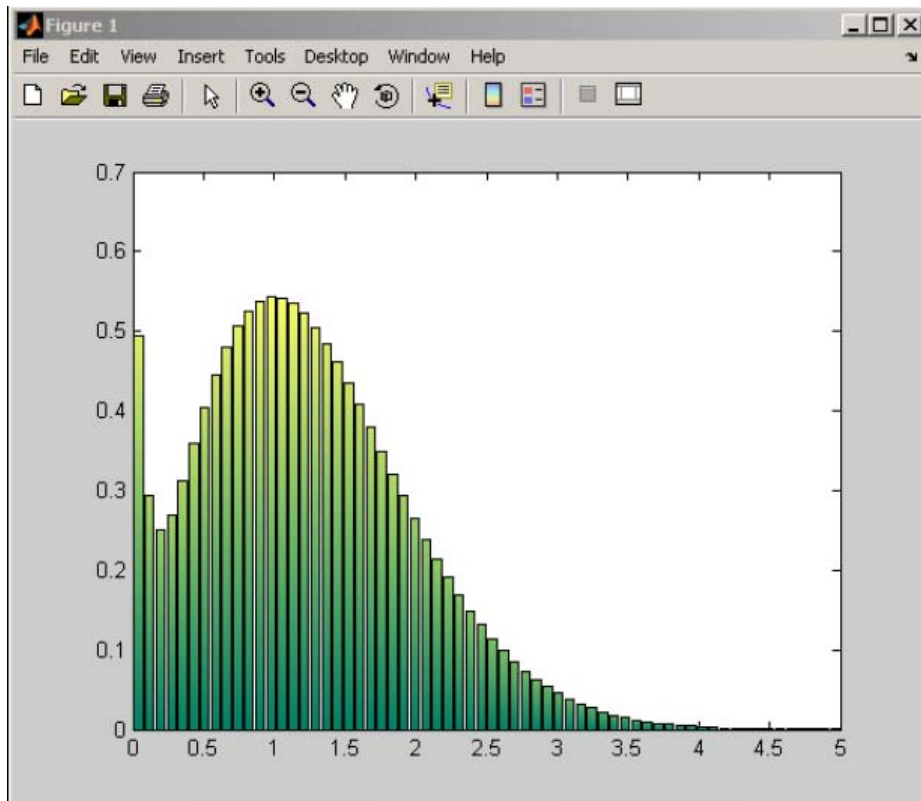


Fig. 52 - M-346 Analytical methodologies development – example of PDF generation for buffet analysis.

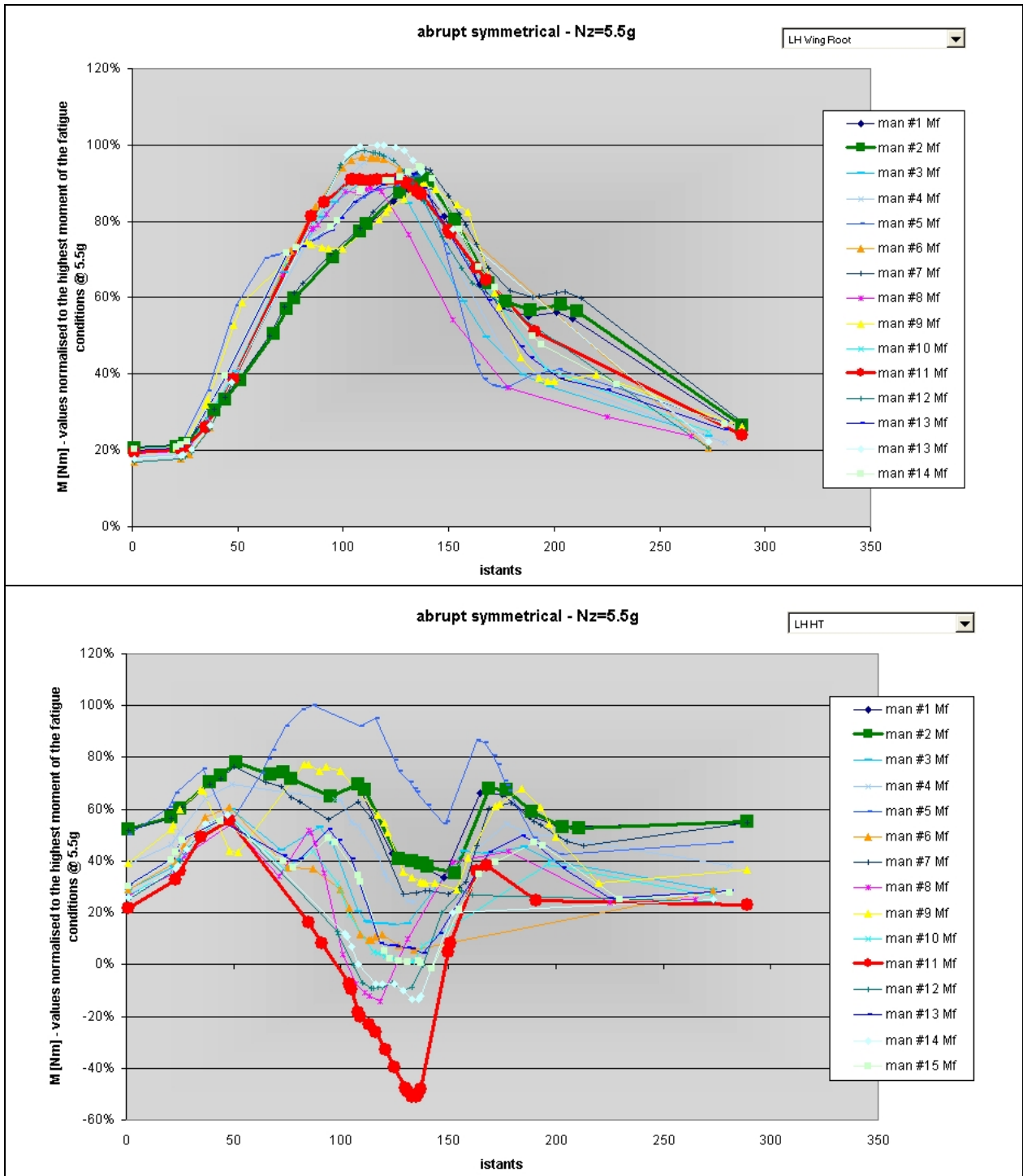


Fig. 53 – M-346 Structural Durability and Damage Tolerance assessment – example of choice of significant conditions to be loaded on the FE model



Fig. 54 - First flight of the Sky-Y unmanned aerial system.

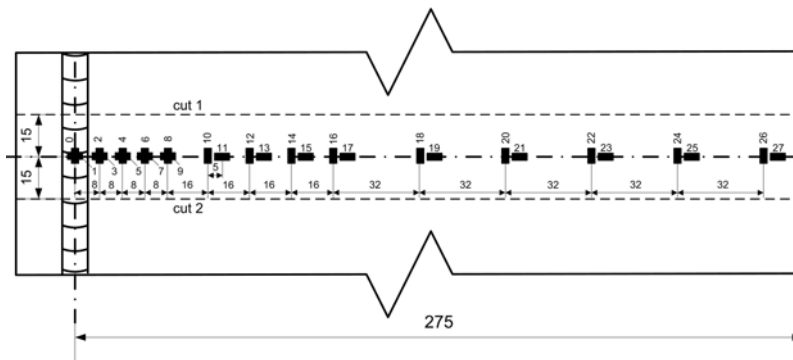


Fig. 55 – Strain gauges map for measurement of residual stresses.

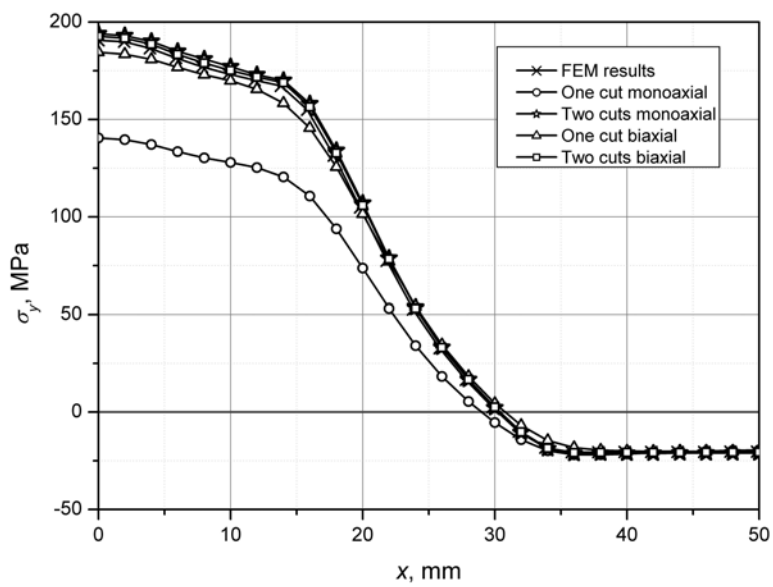


Fig. 56 – Numerical results of residual stress distribution in a butt-welded plate.

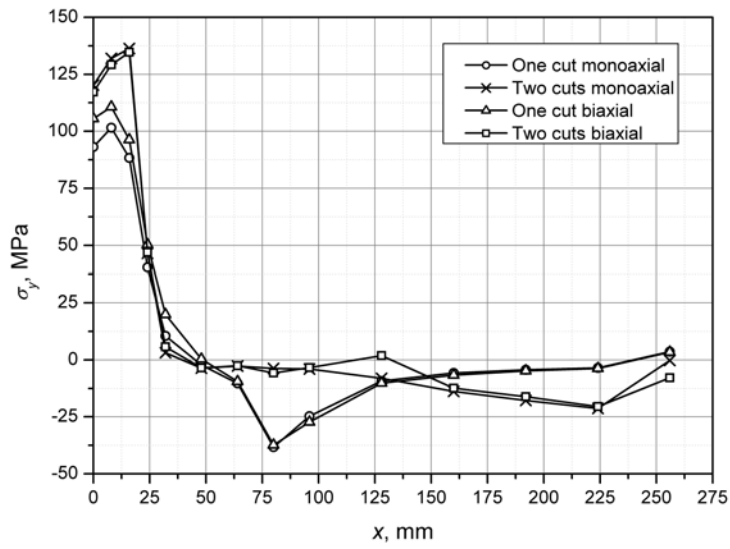


Fig. 57 – Experimental results of residual stress distribution in a butt-welded plate.

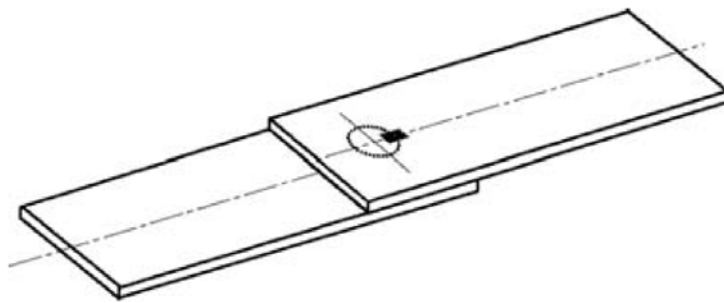


Fig. 58 – Position of the strain gauge in a butt-welded plate

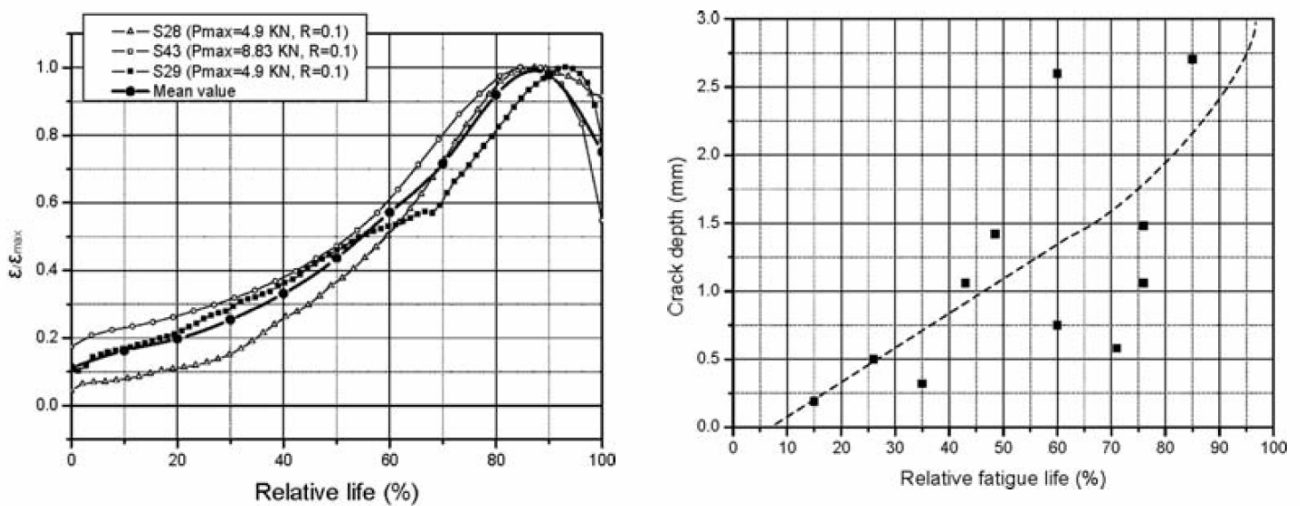


Fig. 59 – Non-dimensional strain gauge output (left) and Crack depth as a function of relative life (right).